Est. 1841 | YORK ST JOHN UNIVERSITY

Ibrahim, Zear, Money, Arthur G, Atwal, Anita and Spiliotopoulou, Georgia (2026) OT-Vision: A 3D depth sensing mobile application to aid clinician-led home environment assessments for falls prevention. Technology and Health Care.

Downloaded from: https://ray.yorksj.ac.uk/id/eprint/16239/

The version presented here may differ from the published version or version of record. If you intend to cite from the work you are advised to consult the publisher's version: https://doi.org/10.1177/09287329261498665

Research at York St John (RaY) is an institutional repository. It supports the principles of open access by making the research outputs of the University available in digital form. Copyright of the items stored in RaY reside with the authors and/or other copyright owners. Users may access full text items free of charge, and may download a copy for private study or non-commercial research. For further reuse terms, see licence terms governing individual outputs. Institutional Repositories Policy Statement

RaY

Research at the University of York St John

For more information please contact RaY at ray@yorksj.ac.uk

Check for updates

Original research article

OT-Vision: A 3D depth sensing mobile application to aid clinician-led home environment assessments for falls prevention

Technology and Health Care
1–31
© The Author(s) 2026
Article reuse guidelines:
sagepub.com/journals-permissions
DOI: 10.1177/09287329261498665
journals.sagepub.com/home/thc
Sage | IOS Press

Zear Ibrahim[1], Arthur G Money[1], Anita Atwal[2] and Georgia Spiliotopoulou[3]

Abstract

Background: Accurate measurement of the home environment is a critical component of clinician-led falls-risk assessment in occupational therapy. However, traditional paper-based measurement approaches can be time-consuming and may introduce variability, particularly under real-world conditions. Advances in mobile depth-sensing technologies provide new opportunities to support clinicians during in-home assessment tasks.

Objective: This paper introduces OT-Vision, a mobile application integrating depth-perception for point-to-point measurement, designed to assist occupational therapists in performing falls-risk assessments within the home.

Methods: A within-subjects counterbalanced mixed-methods design was employed with 37 trainee and practising occupational therapists within controlled simulation environments. OT-Vision was compared with the standard paper-based measurement booklet with respect to measurement bias, accuracy, and task completion time. Usability and user experiences were evaluated via the System Usability Scale and semi-structured interviews.

Results: OT-Vision demonstrated broadly comparable levels of measurement bias compared to the paper-based guidance and modestly greater measurement accuracy, with significantly lower absolute measurement error for two items, following Holm–Bonferroni correction. Participants completed most measurement tasks more efficiently using OT-Vision, and usability scores were higher for OT-Vision versus the paper-based booklet. Qualitative findings indicated perceived benefits in workflow efficiency and measurement confidence, alongside challenges associated with reflective surfaces and adoption within established practice.

Conclusions: The findings suggest that mobile depth perception-enabled measurement applications such as OT-Vision may support more efficient and reliable measurement during home environment falls-risk assessments. While further refinement is required to address interaction and surface-related challenges, OT-Vision shows promise as a digital tool to support contemporary occupational therapy assessment practices.

Keywords

Home environment measurement, falls prevention assessment, augmented reality, depth-sensing technology, occupational therapy, digital health, mobile measurement tools, mHealth, virtual reality

Received: 30 March 2026; accepted: 3 October 2026

1 Background

Population ageing represents a major global demographic shift and is associated with increasing numbers of older adults seeking to remain living independently in their own homes for longer periods.[1] Similar trends are evident in the UK, where increased longevity has contributed to sustained growth in demand for health and social care services, occurring alongside

[1]Department of Computer Science, Brunel University of London, Uxbridge, UK
[2]School of Science, Technology and Health, York St John University, York, UK
[3]Department of Clinical Sciences, Brunel University of London, Uxbridge, UK

Corresponding author:
Arthur G Money, Department of Computer Science, Brunel University of London, Uxbridge UB8 3PH, UK.
Email: arthur.money@brunel.ac.uk

continued constraints on available public resources.[2] Within this context, the adoption of innovative Information and Communication Technologies (ICTs) has been widely identified as a key strategy for supporting more efficient and person-centred models of healthcare delivery.[3,4] Reflecting this position, the UK government has articulated a clear commitment to digital transformation in healthcare through initiatives including *Going Paperless by 2018*,[5] the *Five Year Forward View*,[6] and the *NHS Long Term Plan*.[7,8] However, despite this strategic emphasis, the extent to which ICTs have been effectively implemented across clinical practice remains variable, and occupational therapy**,** in particular, has seen limited uptake of digital tools to support falls prevention interventions, clinical decision-making, and home assessment processes.

Occupational therapy falls prevention is subject to further pressures arising from workforce limitations, as worldwide shortfalls in trained practitioners continue to challenge service delivery. Falls-related injuries also impose a considerable and escalating burden on healthcare systems, particularly in ageing populations. In the UK, falls represent the primary cause of injury-related mortality in adults over 65 and are linked to an estimated annual NHS cost of £4.4 billion[9] with around 30% of independently living older adults sustaining at least one fall annually within the home.[10] These patterns emphasise the demand for efficient, technology-enabled approaches that support clinicians in accurately identifying and mitigating environmental falls hazards.

One of the primary falls prevention strategies in occupational therapy centres on adapting the home environment through purposeful modifications and the fitting of assistive equipment (AE), including stair rails, grab bars, and raised seating. Home visits conducted by occupational therapists are integral to this process, during which thorough evaluations of environmental risk factors are performed. When appropriately prescribed and installed, home adaptations can lower falls risk, reduce long-term care expenditure, and enhance quality of life by supporting older adults to remain at home. Notwithstanding these benefits, a significant proportion of installed AE is subsequently abandoned. This has been linked in part to inaccuracies arising during home environment assessments, most notably measurement errors, which may compromise the suitability of recommended interventions and their associated outcomes.[11]

1.1 Home environment falls risk assessments for assistive equipment prescription and installation

Before home modifications can be implemented, occupational therapists (OTs) undertake comprehensive falls risk assessments that consider both intrinsic factors (e.g. health conditions, medication use, vision, balance, and mobility) and extrinsic factors relating to features of the home environment. Evaluating the interaction between these factors, often conceptualised within occupational therapy as *occupation*, enables OTs to identify potential risks, formulate appropriate interventions, and prescribe AE tailored to the individual's functional needs.

In current practice, home environment falls risk assessments (HEFRAs) are largely supported by basic measurement tools, most commonly retractable tape measures and paper-based measurement guides. These guides support OTs in obtaining measurements for key items of household furniture, including beds, baths, chairs, stairs, and toilets, and relevant anthropometric measures such as popliteal height,[11] typically presenting two-dimensional (2D) illustrations with annotated measurement points to assist accurate AE prescription and installation.[12–14] Despite the availability of such guidance, rates of AE abandonment remain high, with almost one-third of installed equipment ultimately not retained by users.[14–16]

Measurement-related inaccuracies during HEFRAs are frequently cited as a contributing factor to AE abandonment, resulting in equipment poorly fitted to the individual or the home environment.[17,18] The consequences of abandonment are multifaceted and include reduced independence, diminished quality of life, increased falls risk, and additional pressures on healthcare services and resources.[19,20]

Given these challenges, novel approaches are urgently required that can enhance measurement accuracy and efficiency in home-based assessment practice. Emerging mobile technologies hold considerable promise for enhancing measurement precision and reducing the risk of errors that could result in inappropriate AE prescriptions.

1.2 State of the art technology-enhanced falls risk assessments applications

A growing body of research has examined how digital technologies can improve healthcare assessment and intervention processes, including a shift away from conventional paper-based 2D clinical tools towards interactive three-dimensional (3D) visualisation applications which employ computer-generated graphics, allowing users to select, rotate, and zoom virtual representations, to offer richer visual fidelity and spatial information than traditional 2D tools to support clinical assessment and treatment tasks.[21] 3D visualisation has been shown to improve communication and understanding between patients and clinicians. For example, Jang et al.[22] demonstrated how interactive 3D body models can support patients in expressing pain locations and symptoms more accurately. Similarly, Fall Sensei[23] employs a simulated 3D home environment within an interactive game-based format to educate patients about potential falls hazards.

The potential value of 3D visualisation has also been explored specifically in relation to measurement guidance for HEFRAs.[24] Applications such as Guidetomeasure-OT, designed to support clinicians,[18] and Guidetomeasure-3D, aimed

at patient self-assessment,[25] have reported improvements in efficiency, usability, and measurement accuracy when compared with paper-based equivalents. Qualitative research indicates that occupational therapists view 3D visualisation technologies positively.[17] Related studies using home interior design software[26] and the 3D-MAP application[27] further support more effective collaboration between patients and practitioners, while mobile virtual home visits deployed by the Home Quick application demonstrated comparable measurement accuracy and improved efficiency relative to traditional in-person assessments[28]

A directly related pilot study by Ibrahim et al.[29] introduced PilOT-Measure, a mobile depth-sensing measurement application combining active Time-of-Flight range sensing with a basic point-to-point marker placement function for use during HEFRAs. In a preliminary evaluation with 21 trainee and registered occupational therapists, PilOT-Measure improved task efficiency relative to the paper-based booklet but did not consistently improve measurement bias or improve absolute measurement error; the booklet outperformed PilOT-Measure on measurement accuracy (absolute error) for the majority of measured items. Marker placement in PilOT-Measure relied on a nearest-neighbour search applied directly to the raw, unprocessed 3D point cloud, with no mechanism to correct for sensor noise or to align the marker with the true physical edge of the item being measured. That pilot study identified refinement of marker placement and improvement of measurement consistency as priorities for future development.

Despite these promising findings, existing studies indicate that the accuracy and efficiency gains achieved through 3D visualisation alone remain limited when compared with conventional paper-based approaches[24] As a result, multiple authors have highlighted the need for future research to investigate the integration of mobile 3D depth-sensing camera technologies to further enhance assessment accuracy and clinical support across patient-centred care settings[18,25]

1.3 Augmenting home environment falls risk assessment via mobile interactive depth-sensing technologies

Depth-sensing technologies, also known as range-sensing technologies, enable the acquisition of detailed 3D spatial data characterising physical environments and the objects they contain. Within mobile computing environments, the most widely deployed sensor types are laser-based LiDAR (Light Detection and Ranging) and Infrared (IR) Time-of-Flight (ToF) sensors, most commonly used to generate spatially accurate 3D representations and measurements of real-world environments.[30] These sensors are well suited to mobile deployment due to their relative affordability, reliability, and accuracy, and are increasingly incorporated as standard components in smartphones and tablet devices produced by manufacturers such as Apple Inc. (Cupertino, CA, USA) and Samsung Electronics Co., Ltd (Suwon-si, Gyeonggi-do, South Korea).[31] Depth-sensing functionality has also been incorporated into commercial platforms beyond standard consumer devices, including Kinect (Microsoft Corporation, Redmond, WA, USA),[32] Tango (Google LLC, Mountain View, CA, USA),[33,34] Occipital (Occipital Inc., Boulder, CO, USA),[35,36] and the Huawei AR engine (Huawei Technologies Co., Ltd, Shenzhen, Guangdong, China).[37]

Within occupational therapy and related research domains, depth-sensing technologies, particularly Xbox 360 Kinect sensors, have demonstrated considerable potential. Kinect-based virtual reality (VR) exercise interventions have been shown to enhance motor training and reduce long-term falls risk among older adults.[38] Studies focusing on balance training have reported significant gains in overall balance performance when depth-enabled systems are used to support exercise engagement.[39,40] Beyond falls prevention, depth-sensing technologies have also been applied to rehabilitation, assessment, and monitoring contexts, including posture and balance analysis, where sensor-derived metrics have been shown to correlate strongly with established clinical assessment scores.[41,42] Additional work has demonstrated the feasibility of using depth sensors in post-stroke upper-limb rehabilitation[43] and in longitudinal gait monitoring studies conducted within the home environment.[44] Building upon the findings of Ibrahim et al.,[29] the present study extends the PilOT-Measure prototype by addressing the principal limitation identified during the pilot evaluation: measurement marker placement. Specifically, OT-Vision introduces a point-to-point corrected digital marker placement algorithm that applies depth-map alignment, edge detection, and corrected nearest-neighbour searching to improve marker positioning during home environment falls risk assessments.

In direct response to these findings, the present study introduces a fully implemented point-to-point corrected digital marker placement algorithm. Rather than mapping a user's touch input directly onto the nearest point in the raw 3D point cloud, the algorithm combines depth-map alignment with Sobel-based edge detection to identify the true physical edge of the item nearest to the user's selection, before applying a corrected nearest-neighbour search to anchor the measurement marker to that edge. OT-Vision, incorporating this corrected measurement approach, was developed with the goal of achieving more accurate point-to-point measurement of key household furniture items than is currently achieved using traditional paper-based measurement guidance.

1.4 Research questions

This study is guided by two overarching objectives. First, it introduces OT-Vision, a mobile point-to-point measurement application deployed on a commercially available tablet with integrated depth-perception capabilities, incorporating corrected digital marker placement. The application combines active and passive range-sensing techniques with parallax-based image analysis to support measurement capture during HEFRAs.

Second, the performance of OT-Vision is evaluated through clinician-led trials comparing it with the paper-based measurement booklet that presently constitutes standard practice. The evaluation encompasses measurement accuracy, bias (systematic directional deviation), and efficiency, as well as an exploration of user perceptions and adoption intentions.

Accordingly, the study addresses the following research questions:

RQ1: To what degree does OT-Vision and the paper-based guidance booklet exhibit measurement bias relative to the reference standard?
RQ2: To what degree does OT-Vision enhance the accuracy of recorded measurements, compared to those obtained using the paper-based guidance booklet?
RQ3: What differences, if any, are observed in the time and efficiency of measurement recording when using OT-Vision relative to the paper-based approach?
RQ4: How do users rate the usability of OT-Vision when compared against the paper-based guidance booklet?
RQ5: How do occupational therapists perceive OT-Vision with respect to its utility, constraints, potential use cases, and their intention to integrate the application into clinical practice?

2 OT-Vision: A depth perception enabled home environment falls risk assessment application

This section presents OT-Vision, a mobile depth perception enabled application developed to aid occupational therapy clinicians to take accurate digital measurements as part of the HEFRA process. Section 2.1 presents a full walkthrough of OT-Vision. Section 2.2 presents the full system architecture. Section 2.3 presents the proposed image-processing pipeline and bespoke computer vision correction handler function. The source-code for this can be found on GitHub,[45] and the pseudocode, a language-independent solution, is provided in the Appendix A. Collectively, this work is designed to assist the user by optimising point-to-point measurement marker placement in 3D space and deliver enhanced measurement accuracy through edge detection.

2.1 OT-Vision walk-throughs

This section presents a walk-through of OT-Vision.

2.1.1 Main menu and launch screen. OT-Vision was implemented using the Unity3D development environment enabling cross-platform deployment on mobile devices equipped with integrated Time-of-Flight (ToF) depth-sensing hardware. Such sensors are now standard in flagship smartphones and tablets from Apple,[46,47] Huawei,[48–51] Samsung,[52–55] and others.[56]

When launched, users are presented with a Point-Of-View (POV) camera feed displaying the live environment, with overlaid application control panels for accessing measurement and interaction features shown in Figure 1.

2.1.2 Taking and recording measurements. OT-Vision supports point-to-point measurement capture through the interactive placement of digital measurement markers directly within the live camera view. Markers are augmented into the physical scene and spatially anchored using depth information, allowing multiple measurements to be recorded within the same environment. Figure 2 illustrates the placement of measurement markers and the visualisation of connected point-to-point measurements within the real-world scene.

Prior to recording a measurement, users specify both the household item of interest (for example, bed, bath, chair, popliteal height, stairs, or toilet) and the relevant measurement dimension, such as height, width, or depth. These selections are made via the Measurement Indicator Overlay located within the application's control interface, where item categories and measurement types can be cycled using arrow-based navigation controls. The layout of the Measurement Indicator Overlay and the associated Measurement Controls Overlay is shown in Figure 3.

After selecting the measurement context, the user positions the device so that the target object is visible within the camera view. Measurement markers are then placed by tapping the desired start and end locations on the object. Haptic



Figure 1. Bland-Altman plots (bias and non-parametric limits of agreement) for OT-Vision vs. booklet, by measurement item.

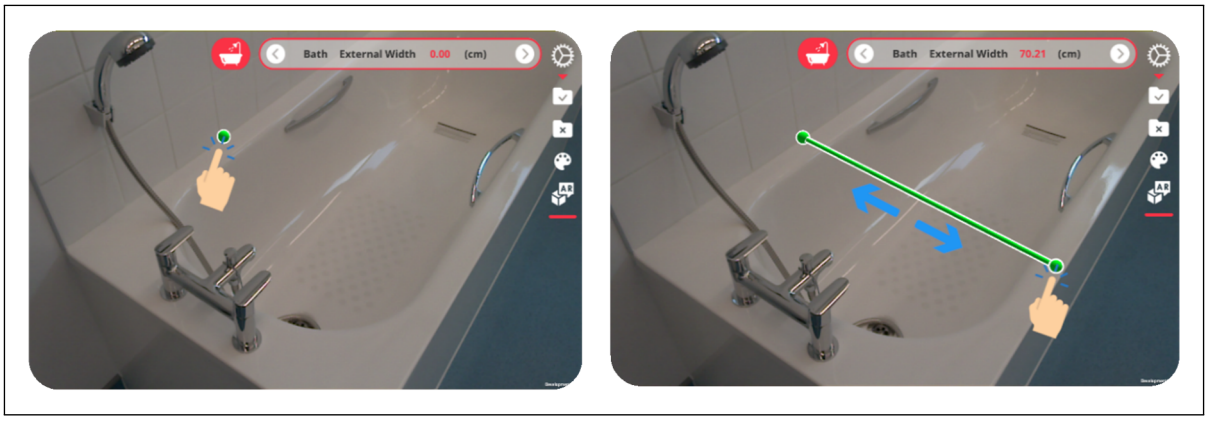


Figure 2. OT-Vision launch screen displaying the application control panel (top and top-right) alongside a live camera feed of the Assisted Daily Living Suite environment.

feedback confirms successful marker placement when the system identifies a valid surface or edge. Once two markers have been positioned, OT-Vision automatically generates a connecting line representing the measured distance and displays the corresponding measurement value, as illustrated in Figure 2.

Measurement values can be displayed in different units, including centimetres, millimetres, or inches, depending on user preference. This process can be repeated for multiple measurement items and dimensions by updating the selection within the Measurement Indicator Overlay and placing additional marker pairs as required. An example set of completed bath measurements captured using OT-Vision is presented in Figure 4.

2.1.3 Optimising measurement marker placement. To support accurate placement of measurement markers in 3D space, OT-Vision generates a 3D depth map of the scene currently in view and employs an edge detection algorithm: the Nearest

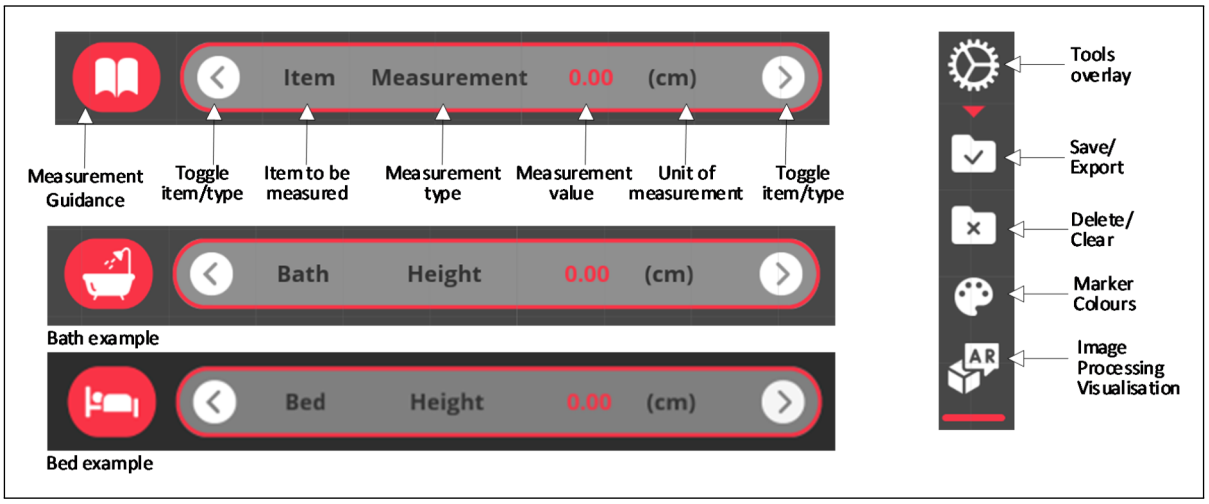


Figure 3. [Left] Placing the first measurement marker, [Right] Placing the second marker with 3D line drawn relative to Time-of-Flight depth for Bath External Width (70.21 cm).

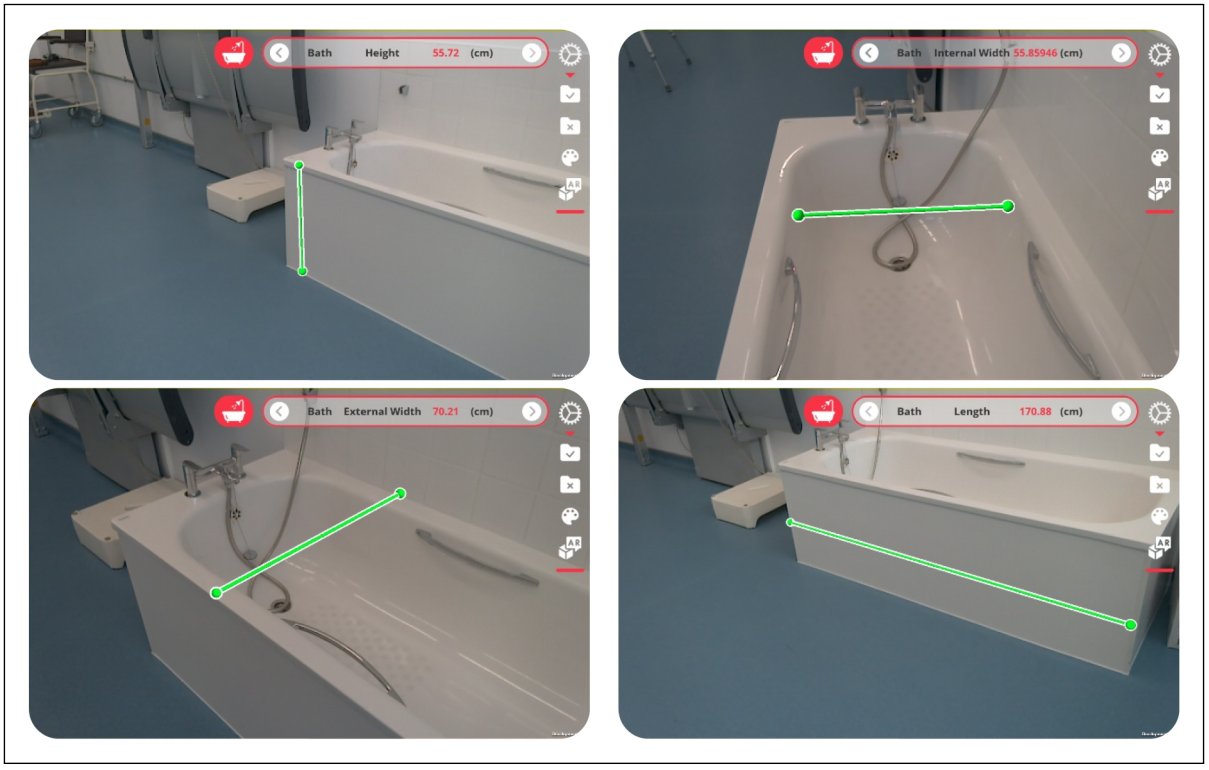


Figure 4. [Left] OT-Vision Measurement Indicator Overlay application control panels including examples toggled for bath height and bed height, [Right] Measurement Controls Overlay.

Neighbour Fixed Radius Linear Search (NNFRLS), described in Section 2.2). It searches the depth map around the area in which the marker has initially been placed with the goal of finding the best candidate edge to place the measurement marker on within the depth map. As HEFRA measurement guidelines require edge-to-edge measurements to be taken (e.g. one edge of bath to the other edge, or the edge of the top stair to edge of the bottom stair), this feature enables measurement markers to be placed in more optimal positions that are in line with the HEFRA measurement task at hand. Figure 5 provides a visualisation of the results of the nearest neighbour search that is carried out and shows the candidate



Figure 5. OT-Vision: Complete Bath Measurement Example. [Top-left] Bath Height (55.72 cm), [Top-right] Bath Internal Width (55.85 cm), [Bottom-left] Bath External Width (70.21 cm), [Bottom-Right] Bath Length (170.88 cm).

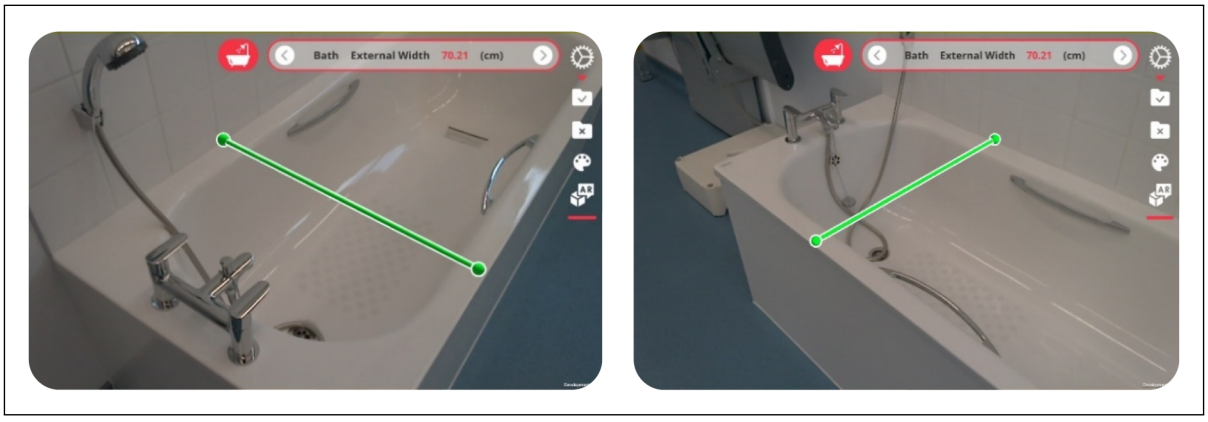


Figure 6. Nearest set of edge vector coordinates calculated around a user's marker placement. [Left] bottom of bath, [Right] top of bath.

edge measurement markers that OT-Vision identifies as a result of deploying the NNFRLS algorithm on the depth map that corresponds with the camera point of view.

Measurement markers and their associated line attachments are embedded within the 3D depth map as interactive 3D object instances, fixed to the vector coordinates within the device's 3D point cloud. Consequently, regardless of changes to the device POV, the markers retain their position.[57,58] Figure 6 illustrates the same measurement markers placed to measure external bath width, but from different points of view. Enabling users to change POV allows them to verify and confirm that the marker placement is as expected.

2.1.4 Managing measurement capture and visual markers. OT-Vision provides integrated mechanisms for storing, modifying, and managing measurement data during a measurement session. Measurement capture is initiated via the *save/export* function, which records the current camera view as a screenshot and stores the associated measurement values. In addition to these primary outputs, supporting data artefacts, including the depth map, edge convolution output, and point-cloud files, are also saved to enable off-device visualisation and further inspection where required. Example data exports are made available through the project's GitHub repository.[45]

Measurement markers and associated data can be removed using the *delete/clear* control within the Measurement Controls Overlay menu, as shown in Figure 3. Each activation of this control removes the most recently placed marker along with its corresponding measurement. In situations where marker placement requires refinement, OT-Vision allows markers to be repositioned after initial placement. Markers can be selected and adjusted directly through touch-based drag interactions, enabling users to optimise their positioning by inspecting marker alignment from multiple viewpoints within the camera view.

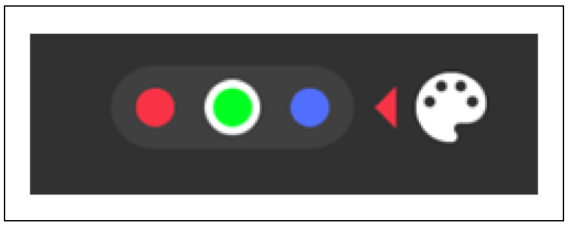


Figure 7. Measurement markers for Bath External Width fixed in 3D space viewed from different POVs with consistent measurement of 70.21 cm.

To support accurate spatial interpretation, the application incorporates visual depth cues that convey distance and marker positioning within the 3D scene. These cues are achieved through a combination of object occlusion and dynamic marker scaling, whereby markers appear smaller when positioned further from the device. This provides immediate visual feedback regarding depth and relative placement within the environment. In addition, users may customise the appearance of markers and connecting lines using the colour palette feature. The available marker and connector colour options are illustrated in Figure 7.

2.1.5 Onboarding instructions. Selecting the booklet icon on the far left-hand side of the Measurement Indicator Overlay menu triggers an on-boarding instructional video which is played to the user. This video explains the main features of the application, the menu features, and the principles of optimal measurement marker placement. It delivers bespoke animated measurement instructions in 3D video format for five key fittings (i.e. bath, bed, chair, stairs, toilet) that are required to carry out a full HEFRA. The measurement guidance icon is context aware, and hence, the video instruction that plays changes depending on which item has been toggled into focus. For example, if the bed is in focus, clicking on the bed icon will trigger a measurement instruction video for the bed to be played.

2.2 System design and processing pipeline

This section presents the architectural design of OT-Vision.

It describes the integration of the *Computer Vision Handler*, which applies established image processing techniques to implement the *Point-To-Point Corrected Digital Measurement (PPCDM)* approach. The system is designed to operate on a *Mobile Depth Sensing and Motion Tracking Device (MDSMTD)* and to support clinician-led measurement activities during HEFRAs. Figure 8 provides an overview of the system architecture and illustrates how *PPCDM* is applied within this mobile sensing context.

During operation, the device camera continuously captures visual data from the physical environment, while on-board motion sensing components monitor device movement. *Motion Sensors* (MS), in conjunction with *Visual Inertial Odometry* (VIO), use data from the *Gyroscope* and *Accelerometer* to estimate device pose and trajectory. These processes trigger asynchronous data callbacks within the device 3D and user experience (UX) application programming interfaces (APIs). As the fisheye, RGB, and *Time-of-Flight* sensors operate at differing sampling frequencies, incoming sensor streams are independently time-stamped before being synchronised for further processing. Using this fused sensor data, the *Device 3D API* constructs a homogeneous four-dimensional point cloud representation (X, Y, Z, W) of the surrounding environment. Similar architectural patterns and interpolation strategies have been reported in related work and could be adopted to redeploy this approach in other systems.[30,37,59–62]

Interaction with the OT-Vision system is primarily mediated through 2D point selection on the touchscreen. When a valid selection is detected, control is passed to the *Measurement Controller*, which invokes the *Computer Vision Handler* to process the user input and identify relevant 3D features within the point cloud. Although new 3D data continue to stream asynchronously in the background, computational processing is initiated only in response to user interaction. During this process, 2D pixel coordinates associated with the user's selection are interpolated and mapped to the nearest corresponding 3D points. The *Measurement GUI* is subsequently updated using appropriate textures and shaders, while touch events are managed by the *Event-Handler* and task coordination is handled by the *Measurement Controller*. This interaction model supports accurate placement of 3D measurement markers and the subsequent recording of measurement data.

To support *PPCDM* functionality, the *Computer Vision Handler* operates through a three-phase processing pipeline:

Phase 1: The *Depth Map Computation logic*, continuously receives point cloud, pose, and camera intrinsic data. De-homogenized 4D points, 3D indices, and depth map pixel indexes are stored in the Coordinate Handler for later use.

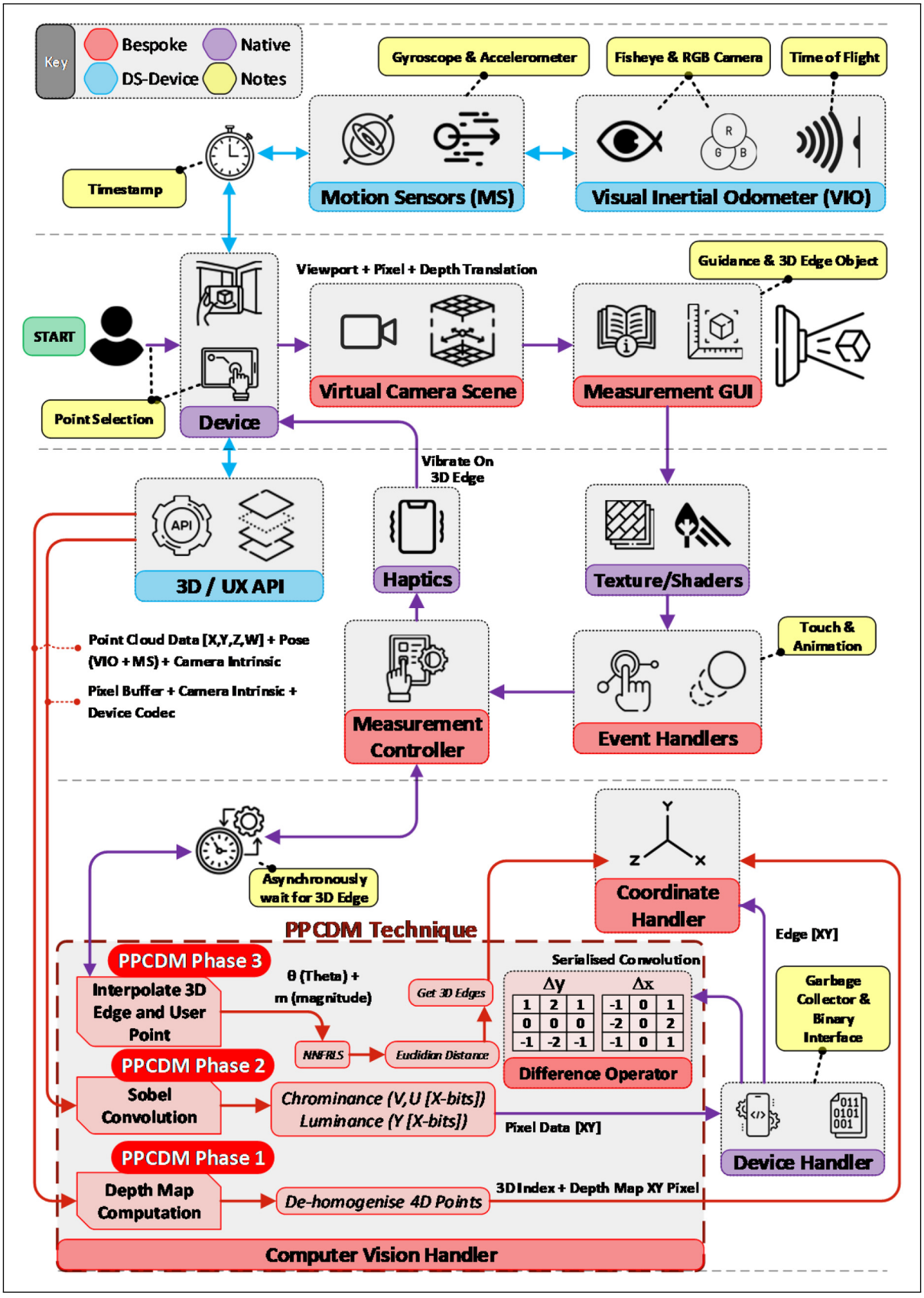


Figure 8. OT-Vision marker colour adjustment options.

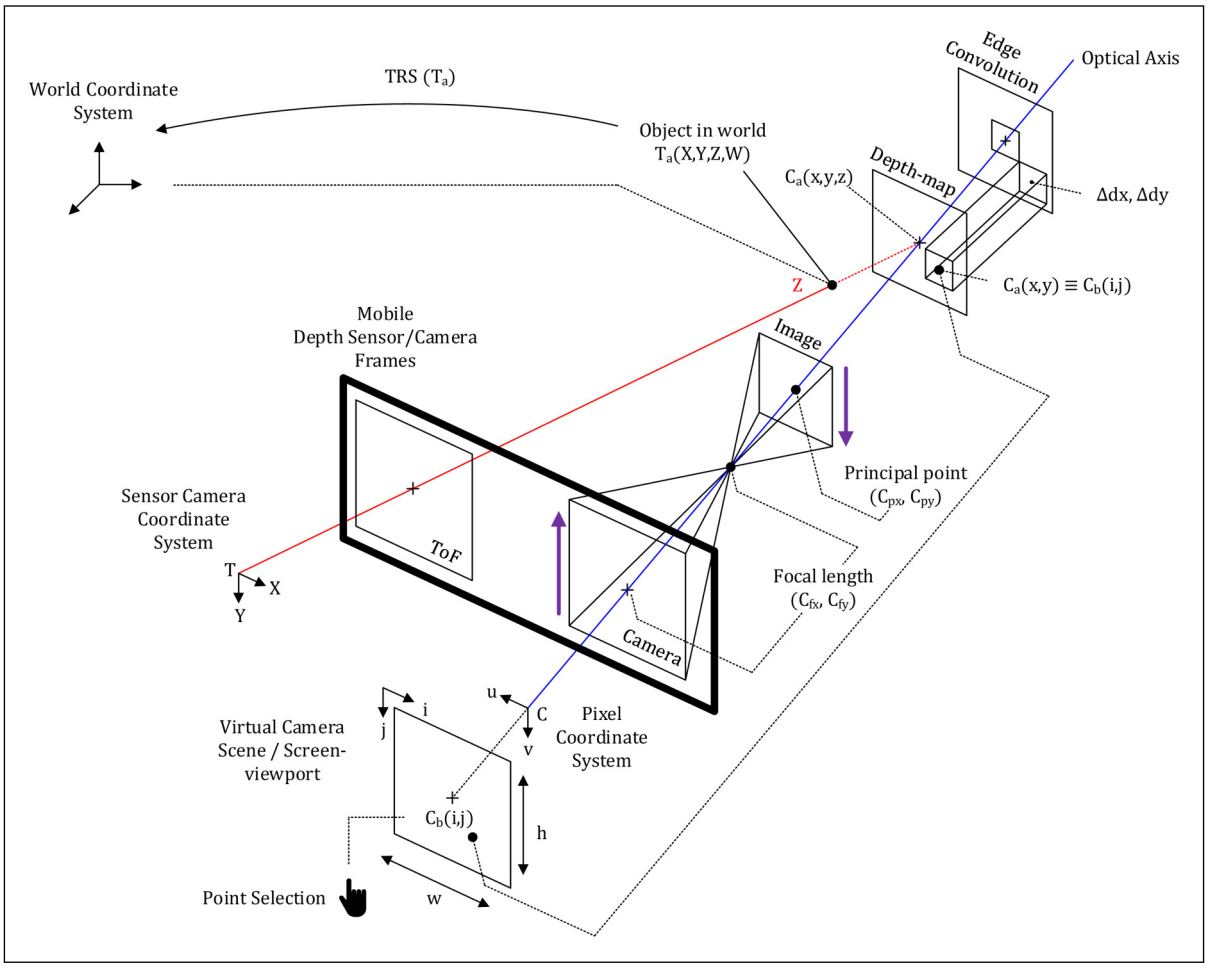


Figure 9. OT-Vision system architecture.

Phase 2: The *Sobel Convolution*, applies a difference operator to pixels around the 2D Point Selection, using pixel buffers and intrinsic values to map the 2D edges against the 3D Depth Map coordinates
Phase 3: Matches these 3D edges to the user's selection by applying a NNFRLS using Euclidean distance as the proximity measure.

2.3 Computer vision handler

This section presents the algorithmic design of the OT-Vision system.

The *Computer Vision Handler* operates on a standard point-cloud as produced by commercial MDSMTDs[30,62,63] in 4D homogenous coordinate format (X, Y, Z, W). Figure 9 presents the geometric model showing how 2D image data and 3D depth data from the device are aligned.

In Figure 9, we adopt the standard RGB-D mapping methods to convert the point-cloud into a depth map. This alignment ensures that there are no projection errors (hovering markers, shifted edges) when referencing data between the colour camera and the depth sensor.[57,64] The subsequent Sections 2.3.1, 2.3.2 and 2.3.3 build on this model and provide the computation necessary to improve the user's 2D Point Selection $C_b(i,\ j)$ by mapping it to the corresponding 3D edge coordinate $C_a(x,\ y)$. The language-independent pseudocode can be found in Sections 10.1, 10.2, and 10.3.

2.3.1 Phase 1 – depth map computation. In the first instance, as shown in Figure 9, for each point T_a in the point cloud, we extract vertices as simple $X,\ Y,\ Z$ values that are stored sequentially:

$$T_a(X) = pointcloud[i \times 4] \qquad (1, \text{Code})$$

$$T_a(Y) = pointcloud[i \times 4 + 1] \quad (2, \text{Code})$$

$$T_a(Z) = pointcloud[i \times 4 + 2] \quad (3, \text{Code})$$

Where $T_a(X)$, $T_a(Y)$ and $T_a(Z)$ represent homogeneous float values describing a vertex in 3D space. The index position i increments across the array, giving connected vertices for each point.

To map each point into the RGB image plane, we apply a perspective projection using the intrinsic camera parameters for focal lengths (C_{fx} and C_{fy}), and principal points (C_{px} and C_{py}) using standard affine transformation functions.[65–67]

$$C_a(x) = C_{fx}\left(\frac{T_a(X)}{T_a(Z)}\right) + C_{px} \quad (4, \text{Code})$$

$$C_a(y) = C_{fy}\left(\frac{T_a(Y)}{T_a(Z)}\right) + C_{py} \quad (5, \text{Code})$$

$$C_a(z) = 255 - \left((T_a(Z) \times 1000) \times \frac{255}{4500}\right) \quad (6, \text{Code})$$

Where $C_a(x)$ and $C_a(y)$ are integer pixel position in the RGB buffer of camera C, and $C_a(z)$ is the depth-coded grayscale value (0–255). For each computation, the depth-map coordinate $C_a(x,\ y)$ corresponds directly to the user's pixel coordinate on the image plane $C_b(i,\ j)$, such that T_a indexes the world coordinate for this 3D vector and $C_a(z)$ provides the associated depth relative to $T_a(Z)$.

2.3.2 Phase 2 – Sobel convolution. The goal of this phase is to identify structural edges in the RGB image around the user's Point Selection, which can then be linked to corresponding 3D features using the Depth Map in Section 2.3.1.

The user's Point Selection $C_b(i,\ j)$ defines our 2D coordinate ($x_{pixel},\ \ y_{pixel}$) in the RGB image. This coordinate serves as the centre of a local search window used for edge detection. Rather than processing the entire image, our algorithm restricts computation to a square neighbourhood with radius r thereby reducing computational complexity. Using interval boundary notation, our reduced iteration space is defined as:

$$i \in [x_{pixel} - r,\ x_{pixel} + r), \quad j \in [y_{pixel} - r,\ y_{pixel} + r) \quad (7, \text{Code})$$

Where r is a 100-pixel adjustable parameter. This is based on tactile sensing research, where the average pointer finger size was 16–20 mm (45–57 pixels); this value is doubled for effective touch-based experience.[68] Then for each iteration in this local neighbourhood, we extract the corresponding position in the one-dimensional image buffer:

$$C_b(i,\ j) = (j \times w) + i \quad (8, \text{Code})$$

Where w denotes the image width (stride) of pixels in camera (C). This buffer index is used to retrieve pixel luminance values, after which a Sobel convolution is applied. Note that instead of OpenCV's Sobel, which introduces unnecessary library overhead on a mobile platform, we directly implement the 3×3 Sobel masks:

$$\Delta x = \begin{matrix} -1 & 0 & +1 \\ -2 & 0 & +2, \\ -1 & 0 & +1 \end{matrix} \quad \Delta y = \begin{matrix} -1 & -2 & -1 \\ 0 & 0 & 0 \\ +1 & +2 & +1 \end{matrix} \quad (9, \text{Code})$$

For each pixel $C_b(i,\ j)$, we then compute the squared gradient magnitude as the Euclidean response:

$$m = \Delta dx^2 + \Delta dy^2 \quad (10, \text{Code})$$

Here, Δdx and Δdy denote the horizontal and vertical Sobel responses obtained by convolving the corresponding 3×3 kernels with the local image neighbourhood.

2.3.3 Phase 3 – 2D to 3D edge and user point mapping. In this last phase, we use the depth map and edge coordinates from Sections 2.3.1 and 2.3.2 to find the nearest 3D edge based on the users Point Selection. At this stage, the Point Selection $C_b(i,\ j)$ corresponds ($\equiv$) to the Depth-map pixel $C_a(x,\ y)$. The bespoke *Coordinate Handler*[45] also contains the matching point cloud index T_a World Coordinate System.

2.3.4 Implementation parameters. The proposed image-processing pipeline and bespoke computer vision correction handler adopt several key parameter choices grounded in standard practices for ToF depth sensing and video processing. The ToF depth sensor in this study (Google Tango) specifies an effective range of 4.5 meters in typical indoor environments,[69] and is further corroborated in other modern frameworks using ToF such as ARCore,[30] and Huawei AR Engine.[63] This value is used to normalise depth to 8-bit grayscale for visualisation and edge filtering. For occupational therapy home assessment, this range encompasses typical measurement scenarios (furniture dimensions, doorway widths, spatial barriers). Additionally, we allocate a point cloud buffer of 30,000 points per frame as a conservative upper bound to accommodate limited on-device hardware capabilities. Typical ToF depth sensor resolutions (640×480 or equivalent) generate point clouds in the range of 30,000–200,000 points.[70,71] We also apply conversion from the standard YUV (NV21) image buffer to RGB using Microsoft's recommended 8-bit YUV formats specification.[72,73] For edge detection, we set the Sobel threshold at 1024, which is approximately 90% of the maximum gradient magnitude that the Sobel-Feldman algorithm can return (Gx_max = 1020 for 8-bit images). It helps to suppress noise while preserving measurement-relevant geometry.

3 Study design and methods

This section outlines how the study was conducted, including the procedures used to collect data and the methods used for analysis.

3.1 Study sample and recruitment

The study involved thirty-seven trainee and registered occupational therapists (OTs). Recruitment was conducted through local NHS trusts and university-based OT training programmes, with further invitations circulated via occupational therapy communities on Facebook, LinkedIn, and academic intranets serving home adaptations professionals.[74] Eligibility criteria required participants to demonstrate familiarity with smartphone-enabled devices including tablet computers and mobile phones, to have relevant experience in assistive equipment provision and/or home visit assessment, and to be proficient English speakers. Among the 37 participants, 32 identified as female and five as male. Whilst this reflects a gender imbalance, it is consistent with the wider demographic profile of the occupational therapy workforce, which is predominantly female.[75,76] The mean age of participants was 30 years (SD = 5.99), with ages ranging from 21 to 44 years. Nineteen participants were OT trainees, including five in their first year of training, 12 in their second year, and two in their third year. The remaining 18 participants were qualified and practising OTs. Among these, two had more than 10 years of professional experience, 10 had between five and nine years of experience, three had four years of experience, and three had three years of experience.

3.2 Study protocol and measurement procedures

A counterbalanced within-subjects mixed-methods design was used to collect study data. The study was conducted in controlled Assisted Daily Living (ADL) simulation environments. Each ADL suite included a bedroom, bathroom, full-length stairs, and all items of living equipment referenced within the measurement guidance booklet. To support verification and validity, 'true' reference measurements were established for all items prior to participant trials.[77] Reference values were established using a consensus reference standard. Five experienced occupational therapists independently measured each item following an established evidence-based paper-based measurement protocol that has been empirically evaluated within occupational therapy practice.[14] Measurements were subsequently reviewed collectively, and a single representative value was agreed through expert consensus. As the consensus reference was derived using the same paper-based measurement protocol evaluated as the comparator, any systematic measurement error inherent to this approach may also be reflected in the reference measurements and should therefore be considered when interpreting the comparative measurement results. Such expert panel approaches are recognised as acceptable reference standards when no objective criterion standard exists.[78,79]. All participants provided informed consent prior to data collection. At the outset of each session, participants received a brief demonstration of both measurement guidance tools (OT-Vision and the paper-based booklet) and were given time to familiarise themselves with the ADL environment. Familiarisation was standardised, allowing participants approximately 5 min to practise one non-scored measurement task using each tool before the formal trial.

This ensured that all participants had equivalent exposure to both measurement approaches prior to testing. The order of tool presentation was counterbalanced across participants to minimise potential learning and order effects associated with repeated measurement tasks. Each participant was then given a tape measure alongside one of the measurement guidance tools and required to complete the specified measurements. The time taken for each measurement task was logged. Following the measurement task, participants filled in a SUS questionnaire,[80] with each item rated on a 5-point scale (1 = strongly disagree; 5 = strongly agree). Participants then used the alternative tool to repeat the same process. Having finished both conditions and their respective SUS questionnaires, participants took part in a semi-structured post-task interview. These interviews examined participants' views on the utility, challenges, and opportunities of each measurement approach, and were audio-recorded and transcribed verbatim.

4 Data analysis

All quantitative analyses were performed using IBM SPSS Statistics Version 29.0.0. The dataset comprised measurement recordings, completion time data, and responses to the SUS questionnaire. Measurement error was defined as the difference between a participant's recorded value and the corresponding reference measurement. Measurement bias (RQ1) was assessed using one-sample Wilcoxon signed-rank tests on signed error to establish whether median errors deviated significantly from zero for each tool, indicating systematic directional bias. Measurement accuracy across tools (RQ2) was evaluated via a direct paired comparison of absolute error values using a Wilcoxon signed-rank test on related samples. Non-parametric procedures were selected for these analyses, as the measurement error data did not satisfy normality assumptions.

Differences in task completion times (RQ3) were analysed using paired sample t-tests, as inspection of skewness (range = −0.34 to 0.36) and kurtosis (range = −1.27 to −0.64) values confirmed that completion time data were approximately normally distributed across all measurement items, consistent with the accepted ±2 thresholds, as recommended by.[81] Paired sample t-tests were also used to compare individual SUS item responses and SUS subscale scores (RQ4), including Usability (items 1–3 and 5–9) and Learnability (items 4 and 10),[80] as skewness (range = −1.72 to 0.02) and kurtosis (range = −1.04 to 2.06) values were within acceptable limits across SUS items, with only one item marginally exceeding the ±2 kurtosis threshold (Item 7 OT-Vision: kurtosis = 2.06), a deviation not considered sufficient to violate the assumption of approximate normality.[81] Overall SUS scores were calculated for each condition and interpreted using established adjective descriptors, acceptability ranges, and school grading scales derived from baseline data from over 3000 software applications.[80] A paired-samples t-test was also used to compare overall SUS scores between conditions as the headline usability outcome for RQ4. Alongside test statistics, 95% confidence intervals and Holm-Bonferroni-corrected p-values (applied within each family of related comparisons) are reported where appropriate.[81]

Interview data pertaining to RQ5 were examined through a reflexive Thematic Template Analysis framework.[82,83] Both inductive (data-driven) and deductive (theory-driven) coding strategies were employed.[84,85] A preliminary coding template was developed drawing on the Unified Theory of Acceptance and Use of Technology (UTAUT),[86] incorporating Performance Expectancy (PE), Effort Expectancy (EE), and Social Influence (SI) as relevant technology adoption constructs. The data were then reviewed iteratively, with coded segments progressively consolidated into broader thematic categories. Two researchers independently engaged with the interview transcripts, generating initial codes and identifying patterns of meaning. Through successive cycles of discussion and refinement, the coding template and associated themes were reviewed and developed collaboratively to enhance interpretative depth and transparency. Memo writing and cross-case comparisons were used throughout the analytic process to support thematic coherence and consistency. The coding framework was refined iteratively until no substantively new themes emerged from the data. Formal inter-coder reliability statistics were not calculated, consistent with contemporary guidance for reflexive qualitative analysis, which conceptualises coding as a process of interpretation and meaning-making rather than a test of coder agreement.[83] The final thematic framework was shaped by a contextual constructivist stance, acknowledging that the interpretation of data is influenced by the context of its production and analysis.[84,87].

5 Study results

5.1 Bias of recorded measurements

Measurement bias, operationalised as signed measurement error, was used to assess systematic directional deviation relative to the reference measurement. Median signed error values were calculated by determining the difference between participant-recorded measurements and the corresponding reference values for each tool, retaining the direction of any deviation to identify systematic over- or under-estimation. A comparison of the resulting error distributions for OT-Vision and the booklet is presented in Table 1.

Table 1. Measurement bias (signed error) for booklet and OT-Vision.

		OT-Vision					Booklet					
	True Md (cm)	Md (cm)	Md Diff. (cm) [95% CI]	Z	Sig	Adj.p	Md (cm)	Md Diff. (cm) [95% CI]	Z	Sig	Adj.Sig.	df
Bath												
Height	45.58	45.56	0.02[−1.11, 0.29]	−1.501	0.133	0.947	45.75	−0.17[−0.42, 0.08]	−0.008	0.994	1.000	36
Int W.	57.60	57.52	0.08[−0.16, 0.53]	0.769	0.442	1.000	57.00	0.60[0.00, 1.60]	2.664	0.008*	0.067	36
Length	166.57	166.81	−0.24[−0.42, 0.23]	−1.388	0.165	1.000	167.00	−0.43[−0.43, −0.13]	−2.184	0.029*	0.211	36
Ext W.	69.67	69.80	−0.13[−0.76, 0.37]	−1.147	0.252	1.000	70.00	−0.33[−0.33, −0.33]	−3.392	0.001*	0.007*	36
Bed												
Height	53.65	53.14	0.51[0.21, 0.83]	3.130	0.002*	0.018*	54.00	−0.35[−1.35, 1.65]	0.279	0.780	1.000	36
Chair												
Height	45.60	45.55	0.05[−0.39, 0.34]	−0.158	0.874	1.000	45.50	0.10[−1.50, 0.40]	−1.578	0.115	0.698	36
Depth	44.50	44.71	−0.21[−1.03, −0.06]	−3.441	0.001*	0.006*	44.00	0.50[−0.50, 1.90]	−1.345	0.179	0.907	36
Width	42.35	42.59	−0.24[−0.59, 0.21]	−1.637	0.102	0.826	42.10	0.25[−0.15, 0.45]	0.710	0.478	1.000	36
Toilet												
Height A	48.75	48.90	−0.15[−0.59, 0.65]	0.204	0.839	1.000	48.00	0.75[0.75, 0.75]	3.831	0.000*	0.001*	36
Height B	46.40	46.44	−0.04[−0.52, 0.29]	−0.121	0.904	1.000	45.50	0.90[0.40, 0.90]	3.276	0.001*	0.010*	36
Stairs												
Length	85.00	85.21	−0.21[−0.56, −0.03]	−2.927	0.003*	0.029*	85.09	−0.09[−0.50, 0.00]	−1.063	0.288	1.000	36

Note: * Statistically significant at <0.05 level. Adj. Sig = Holm-Bonferroni corrected *p*-value, applied within family of 11 comparisons (separately for OT-Vision and Booklet bias).

Table 2. Measurement accuracy (paired comparison of absolute error) for PPCDM and booklet.

	OT-Vision	Booklet	Paired differences						
	Abs. Md.err (cm)	Abs. Md.err (cm)	Md.err.diff (cm) [95% CI]	Df	Z	Sig. (2tail)	Adj.sig.	Effect size (r)	Effect size magnitude
Bath									
Height	0.59	0.42	0.17[−0.14, 0.78]	36	−0.664a	0.507	1.000	0.111	Small
Int W.	0.60	0.61	−0.01[−1.49, 0.49]	36	−2.444b	0.015*	0.120	0.407	Medium
Length	0.53	0.43	0.10[−0.07, 0.46]	36	−0.415a	0.678	1.000	0.069	Trivial
Ext W.	0.67	0.33	0.34[0.14, 0.62]	36	−0.619a	0.536	1.000	0.103	Small
Bed									
Height	0.71	2.15	−1.44[−1.94, −0.69]	36	−3.628b	0.000*	0.003*	0.605	Large
Chair									
Height	0.47	1.10	−0.63[−1.92, 0.01]	36	−2.506b	0.012*	0.120	0.418	Medium
Depth	0.45	1.70	−1.25[−3.29, −0.26]	36	−3.281b	0.001*	0.011*	0.547	Large
Width	0.53	0.85	−0.32[−1.39, 0.27]	36	−2.391b	0.017*	0.120	0.399	Medium
Toilet									
Height A	1.00	0.75	0.25[−0.10, 0.62]	36	−0.015a	0.988	1.000	0.003	Trivial
Height B	0.59	0.90	−0.31[−0.59, −0.02]	36	−1.599b	0.110	0.679	0.267	Small
Stairs									
Length	0.38	0.50	−0.12[−0.70, 0.22]	36	−1.569b	0.117	0.679	0.262	Small

Note: a. Based on negative ranks. b. Based on positive ranks. *Statistically significant at <0.05 level. Adj. Sig. = Holm-Bonferroni corrected p-value, applied within family of 11 comparisons.

One-sample Wilcoxon signed-rank tests comparing OT-Vision measurements against the reference values indicated that eight of the eleven measurement items produced median error values with no statistically significant deviation from the reference measurements at the 0.05 level. These items comprised Bath Height ($z = -1.501$, $p = 0.133$), Bath Internal Width ($z = 0.769$, $p = 0.442$), Bath Length ($z = -1.388$, $p = 0.165$), Bath External Width ($z = -1.147$, $p = 0.252$), Chair Height ($z = -0.158$, $p = 0.874$), Chair Width ($z = -1.637$, $p = 0.102$), Toilet Height A (Floor–Seat) ($z = 0.204$, $p = 0.839$), and Toilet Height B (Floor–Bowl) ($z = -0.121$, $p = 0.904$). For the remaining three items, statistically significant deviations from the reference measurements were observed, indicating significant measurement bias in those cases.

By comparison, median error values for the booklet guidance showed no significant difference from the reference measurements for six of the eleven items, comprising Bath Height ($z = -0.008$, $p = 0.994$), Bed Height ($z = 0.279$, $p = 0.78$), Chair Height ($z = -1.578$, $p = 0.115$), Chair Depth ($z = -1.345$, $p = 0.179$), Chair Width ($z = 0.71$, $p = 0.478$), and Stairs Length ($z = -1.063$, $p = 0.288$). Five measurement items showed statistically significant differences from the reference values, indicating significant measurement bias for those cases when using the booklet.

From a statistical perspective, OT-Vision produced significant bias in three cases, whereas the booklet guidance produced significant bias in five cases.

After Holm-Bonferroni correction within each family of 11 comparisons, all three OT-Vision inaccuracies remained statistically significant (Bed Height, Chair Depth, and Stairs Length; adjusted $p < 0.05$ in each case). For the booklet, two of the five originally significant bias no longer reached significance once corrected (Bath Internal Width, adjusted $p = 0.067$; Bath Length, adjusted $p = 0.211$); the remaining three (Bath External Width, Toilet Height A, and Toilet Height B) remained significant. Overall, the pattern of results indicates broadly comparable levels of measurement bias between tools, with descriptive differences in median signed error favouring OT-Vision for a greater number of measurement items. To further characterise the degree of agreement between the two measurement tools, Bland-Altman analyses (bias and limits of agreement) were additionally conducted for each measurement item; full results are presented in the Appendix B and are broadly consistent with the accuracy findings reported above.

5.2 Accuracy of recorded measurements

Measurement accuracy, assessed here using absolute measurement error, was examined through a direct paired comparison of the absolute measurement errors produced by OT-Vision and the booklet guidance for the same participants. The results of this comparison are summarised in Table 2.

Table 3. Task completion time for ot-vision app vs. booklet.

	OT-Vision Mean (seconds)	Booklet Mean (seconds)	St dev	Mean diff. (seconds) [95% CI]	t	Df	Sig (2-tail)	Adj. sig.
Bath								
Height	11.77	11.02	6.10	−0.75[−2.78, 1.29]	−0.743	36	0.462	0.461
Int W.	11.27	8.96	4.49	−2.31[−3.80, −0.81]	−3.129	36	0.003*	0.021*
Length	10.30	41.63	9.23	31.33[28.26, 34.41]	20.657	36	0.000*	0.000*
Ext W.	6.95	20.65	6.11	13.70[11.67, 15.74]	13.648	36	0.000*	0.000*
Bed								
Height	7.19	15.48	7.50	8.29[5.79, 10.79]	6.724	36	0.000*	0.000*
Chair								
Height	11.79	14.04	7.75	2.26[−0.33, 4.84]	1.772	36	0.085	0.339
Depth	12.57	14.55	7.43	1.99[−0.49, 4.47]	1.628	36	0.112	0.339
Width	10.28	12.95	5.45	2.66[0.84, 4.48]	2.971	36	0.005*	0.026*
Toilet								
Height A	13.30	14.86	5.95	1.56[−0.42, 3.55]	1.599	36	0.119	0.339
Height B	28.47	18.52	13.68	−9.95[−14.51, −5.39]	−4.425	36	0.000*	0.001*
Stairs								
Length	11.00	27.74	7.90	16.74[14.10, 19.37]	12.885	36	0.000*	0.000*

Note: *Statistically significant at <0.05. Adj. Sig. = Holm-Bonferroni corrected p-value, applied within family of 11 comparisons.

Examination of median error differences reveals that OT-Vision yielded lower median error values than the booklet across seven of the eleven measurement items, as evidenced by negative error difference values. These items were Bath Internal Width (Md err.diff = −0.01), Bed Height (Md err.diff = −1.44), Chair Height (Md err.diff = −0.63), Chair Depth (Md err.diff = −1.25), Chair Width (Md err.diff = −0.32), Toilet Height B (Md err.diff = −0.31), and Stairs Length (Md err.diff = −0.12). In each instance, OT-Vision showed descriptively lower absolute error magnitudes compared with the booklet.

Statistical comparison of absolute error values using the Wilcoxon signed-rank test identified five measurement items for which differences between tools were statistically significant. In all five cases, OT-Vision produced more accurate measurements than the booklet. These items were Bath Internal Width ($z = -2.444$, $p = 0.015$, medium effect size), Bed Height ($z = -3.628$, $p = 0$, large effect size), Chair Height ($z = -2.506$, $p = 0.012$, medium effect size), Chair Depth ($z = -3.281$, $p = 0.001$, large effect size), and Chair Width ($z = -2.391$, $p = 0.017$, medium effect size). For seven of the eleven measurement items, z values were based on positive ranks, further indicating that OT-Vision consistently generated lower absolute errors in these cases.

Overall, all statistically significant differences favoured OT-Vision, with no instances in which the booklet guidance significantly outperformed OT-Vision in terms of measurement accuracy.

After Holm-Bonferroni correction, two of the five originally significant differences remained significant (Bed Height, adjusted $p = 0.003$; Chair Depth, adjusted $p = 0.011$); the differences for Bath Internal Width, Chair Height, and Chair Width no longer reached significance once corrected (adjusted $p = 0.120$ for each). Overall, differences in measurement accuracy were modest, although statistically significant differences following correction favoured OT-Vision for two measurement items.

5.3 Measurement task efficiency

Task efficiency was assessed by comparing the time taken to complete measurement tasks using OT-Vision and the booklet guidance. Completion times were recorded in seconds, and results are summarised in Table 3.

Paired samples t-tests revealed statistically significant differences in task completion time for seven of the eleven measurement items. For five of these, participants took considerably longer when using the booklet than OT-Vision, as indicated by positive mean difference values. These items comprised Bath Length ($M.diff = 31.33$, $SD = 9.23$, $p = 0.000$), Bath External Width ($M.diff = 13.70$, $SD = 6.11$, $p = 0.000$), Bed Height ($M.diff = 8.29$, $SD = 7.50$, $p = 0.000$), Stairs Length ($M.diff = 16.74$, $SD = 7.90$, $p = 0.000$), and Chair Height ($M.diff = 2.66$, $SD = 5.45$, $p = 0.005$).

In contrast, two measurement items were completed significantly faster using the booklet guidance. These were Bath Internal Width ($M.diff = -2.31$, $SD = 4.49$, $p = 0.003$) and Toilet Height B ($M.diff = -9.95$, $SD = 13.68$, $p = 0.000$). For

Table 4. OT-Vision app and booklet SUS score comparison.

SUS items	Mean		Gap score [95% CI]	Df	t	Sig. (2-tail)	Adj. sig.
	OT-Vision	Booklet					
S1: I think that I would like to use the app/booklet frequently.	3.95	3.27	0.68[0.17, 1.18]	36	2.721	0.010*	0.080
S2: I found the app/booklet unnecessarily complex.[a]	4.51	3.76	0.76[0.44, 1.08]	36	4.822	0.000*	0.000*
S3: I thought the app/booklet was easy to use.	3.89	3.68	0.22[−0.12, 0.55]	36	1.310	0.198	0.794
S4: I think that I would need the support of a technical person to be able to use the app/booklet.[a]	4.30	4.19	0.11[−0.28, 0.49]	36	0.572	0.571	1.000
S5: I found the various functions in the app/booklet were well integrated.	3.73	3.35	0.38[−0.05, 0.80]	36	1.802	0.080	0.479
S6: I thought there was too much inconsistency in the app/booklet.[a]	3.54	3.70	−0.16[−0.71, 0.39]	36	−0.601	0.552	1.000
S7: I would imagine that most people would learn to use the app/booklet very quickly.	4.00	3.59	0.41[−0.07, 0.88]	36	1.733	0.092	0.479
S8: I found the app/booklet very awkward to use.[a]	3.97	2.95	1.03[0.45, 1.61]	36	3.591	0.001*	0.009*
S9: I felt very confident using the app/booklet.	3.73	3.86	−0.14[−0.51, 0.24]	36	−0.725	0.473	1.000
S10: I needed to learn a lot of things before I could get going with the app/booklet.[a]	4.43	4.08	0.35[−0.02, 0.72]	36	1.924	0.062	0.436
Overall SUS Score	75.14	66.08	9.05[2.95, 15.16]	36	3.006	0.005*	–[b]

aNegative item scores were reversed prior to analysis, such that higher values consistently reflect more favourable responses.
bOverall SUS score is the single headline comparison for RQ4 and is therefore not part of the 10-item correction family; no Holm-Bonferroni adjustment applies.
Note: *Indicates statistically significant at <0.05 level. Adj. Sig. = Holm-Bonferroni corrected *p*-value, applied within family of 10 comparisons.

the remaining four items that did not reach statistical significance, OT-Vision demonstrated shorter completion times in three cases (Toilet Height A, Chair Height, and Chair Depth), as reflected by positive mean difference values.

When aggregated across all measurement tasks, participants completed measurements more quickly using OT-Vision ($M = 453.71$ s) than with the booklet ($M = 674.13$ s), resulting in an overall mean difference of 220.42 s ($p = 0.002$). OT-Vision tended to require more time for measurements involving reflective surfaces (Bath Height, Bath Internal Width, and Toilet Height A), whereas the booklet required the longest completion times for measurements involving larger spatial distances, including Bath Length, Bath External Width, and Stairs Length.

After Holm-Bonferroni correction, all seven originally significant differences in completion time remained statistically significant (adjusted $p < 0.05$ in each case). Overall, the findings suggest that the relative efficiency of each approach depended on the measurement task being performed, with OT-Vision generally associated with shorter completion times for measurements involving larger spatial distances.

5.4 User satisfaction and usability outcomes

Overall usability was assessed using the System Usability Scale (SUS) for both OT-Vision and the booklet guidance. The mean SUS score for the OT-Vision application was 75.14 out of 100 ($SD = 10.93$), which corresponds to a Good descriptive rating, an acceptable usability range, and a Grade B classification according to established SUS interpretation criteria.[80]. The booklet achieved a lower mean SUS score of 66.08 ($SD = 16.20$), corresponding to an OK descriptive rating, a marginal acceptability range, and a Grade C classification. Thus, both approaches achieved usability scores within the acceptable range, although OT-Vision received a higher overall usability rating. A paired-samples t-test confirmed that this difference was statistically significant ($p = 0.005$), with a medium effect size ($r = 0.45$). See Table 4 for full test statistics, including the 95% confidence interval for the difference.

To examine usability in more detail, individual SUS item responses were analysed for both measurement approaches. The results, including item-level mean scores, gap scores, and significance values, are summarised in Table 4; Higher item scores reflect more favourable perceptions of usability and user experience.

OT-Vision achieved mean scores exceeding the 3.00 neutral threshold across all ten SUS items. For the booklet, nine of the ten items surpassed this threshold, with the sole exception being item S8 ($M = 2.95$). This indicates that participants responded positively to OT-Vision across all usability dimensions and generally positively to the booklet.

Across eight of the ten SUS items, OT-Vision achieved higher mean scores than the booklet. The booklet recorded higher mean scores for items S6 and S9; however, neither of these differences reached statistical significance. Statistically

significant differences were observed for three SUS items, and in each case OT-Vision outperformed the booklet. These included item S1, which reflects participants' willingness to use the system more frequently ($p = 0.010$), item S2, which relates to perceived system complexity ($p < 0.000$), and item S8, which captures perceptions of awkwardness during use ($p = 0.001$).

Taken together, these findings indicate that participants reported positive usability experiences with both approaches. OT-Vision received more favourable ratings for perceived complexity (S2) and awkwardness during use (S8), whereas no statistically significant differences were observed for the remaining usability dimensions, including ease of use (S3), learnability (S7 and S10), confidence during use (S9), and functional integration (S5).

After Holm-Bonferroni correction, two of the three originally significant SUS items remained significant (S2, adjusted $p < 0.001$; S8, adjusted $p = 0.009$); the difference for S1 no longer reached significance once corrected (adjusted $p = 0.080$). See Table 4 for 95% confidence intervals and adjusted p-values. These results suggest that perceptions of usability were broadly favourable for both approaches, with the most pronounced differences relating to perceived complexity and ease of interaction.

5.5 Qualitative insights on use, adoption, and implementation

Four overarching themes were identified from the interview data, capturing participants' experiences of OT-Vision and their perspectives on its adoption in practice. The initial three themes (Perceived Performance Benefits; Ease of Use and Interaction Effort; Social and Organisational Influences on Adoption) correspond to constructs within the UTAUT, whilst the fourth theme (Challenges with Reflective Surfaces and Touch Input) arose inductively from the data. Participant quotations are reported using anonymised identifiers, alongside gender and age.

5.5.1 Perceived performance benefits. Participants frequently described OT-Vision as supporting improved measurement performance when compared with paper-based approaches. In particular, the system's edge-detection functionality was perceived as enhancing the precision with which measurement points could be identified and placed.

> I think my measurements have improved using the digital measurement system, especially after learning to locate the points [edges] and place them in the most accurate position. (Participant 10, F, 32)

OT-Vision was also widely associated with efficiency gains, with participants reporting reductions in the time required to complete measurement tasks.

> It's definitely more efficient using the tablet … I can spend less time measuring overall. (Participant 22, F, 29)

> … it'll make it easier, there is far less thinking involved, you don't have to sit there and squint at the tape measure …. I definitely think it'll be quicker. (PP14, F, 28)

Beyond measurement tasks, participants highlighted perceived benefits relating to administrative workload. The ability to digitally capture, store, and manage measurement data was viewed as improving transparency and reducing manual handling of records.

> Having the data sent digitally will remove all these unnecessary steps … good to keep maximum transparency and data retention." (Participant 16, F, 21)

Several participants also suggested that these efficiencies could contribute to reduced stress during home assessments by shortening visits and limiting post-visit documentation demands.

> You're not having to take up as much time … especially if you have to get back and write notes … less stress on that child. (Participant 29, M, 34)

5.5.2 Ease of use and interaction effort. OT-Vision was consistently described as intuitive and straightforward to use. Participants emphasised the benefits of consolidating multiple measurement-related tools and functions within a single application, particularly for less experienced practitioners.

> Everything integrated into one thing . . . I see the advantages of it, especially for newer OTs. (Participant 5, M, 23)

The integration of measurements, guidance, and visual records within one platform was perceived as supporting ease of use and workflow clarity.

> It really streamlines your information with measurements and photos in one place. (Participant 4, M, 27)

Despite these positive perceptions, participants identified areas for improvement. Some noted uncertainty when placing markers, particularly when attempting to ensure that measurement lines were aligned correctly.

> I wasn't always sure I was making a straight line . . . a way to inform the user when the line is straight would be useful. (Participant 12, F, 29)

Suggestions were also made to enhance marker visibility, such as adjusting size or transparency, to support more accurate placement.

> The dot covers the entire edge itself and makes it difficult to see if it's in the right place . . . make it more transparent. (Participant 7, F, 30)

5.5.3 Social and organisation influences on adoption. Social factors were viewed as playing an important role in the adoption of OT-Vision. Participants noted that resistance to change, particularly among more experienced practitioners, could present a barrier to uptake.

> The younger the team, the more open they are . . . OTs who've been in their position a long time . . . roll their eyes at change. (Participant 6, F, 31)

Clinical leadership was identified as a key facilitator, with participants suggesting that endorsement from senior staff could strongly influence adoption decisions within teams.

> Clinical lead level can influence the adoption of this technology quite a lot . . . changes adoption rates. (Participant 28, F, 22)

5.5.4 Challenges with reflective surfaces and touch input. An additional theme emerged relating to challenges associated with reflective surfaces. Participants reported difficulties when placing measurement markers on shiny materials, such as bathroom fixtures. While these issues were often mitigated by adjusting viewing angles, participants suggested that further system support could improve usability in these scenarios.

> Finding a point on the shiny surface was very difficult. (Participant 15, F, 34)

Suggestions included providing clearer on-screen guidance when marker placement fails repeatedly.

> If the user taps the screen several times and no point is placed, then a pop-up to instruct the user on what to do would be helpful. (Participant 16, F, 21)

6 Discussion

This study examined the potential of OT-Vision, a mobile depth perception-enabled measurement application, to support Home HEFRAs. Alongside the presentation of the application architecture and the PPCDM function, the system was evaluated with trainee and practising occupational therapists against the current paper-based measurement guidance. The findings are discussed below in relation to measurement performance, efficiency, usability, and clinicians' perspectives on adoption, with reference to existing research in depth sensing, digital assessment tools, and occupational therapy practice.

Before discussing the individual research questions, it is important to consider the consensus reference standard used to evaluate measurement performance. The reference measurements were established using the same evidence-based paper-based measurement protocol evaluated as the comparator. Consequently, any systematic measurement error inherent to

this approach may also be reflected in the reference measurements, meaning that comparisons with OT-Vision should be interpreted in this context. As such, the evaluation may represent a conservative comparison that has the potential to favour the paper-based booklet should systematic measurement error be present within the comparator.

Regarding measurement bias, the findings demonstrate that OT-Vision achieves levels of systematic directional deviation comparable to conventional paper-based measurement guidance. OT-Vision measurements did not differ significantly from the reference measurements for most measurement items, and following Holm–Bonferroni correction, both OT-Vision and the paper-based booklet demonstrated statistically significant measurement bias for only three of the eleven measurement items, indicating broadly comparable levels of systematic directional bias between the two approaches. These outcomes are consistent with prior work showing that digital measurement tools incorporating 3D visualisation, augmented reality, and virtual reality technologies can match or exceed the accuracy of conventional manual methods. More broadly, ToF depth-sensing technologies have demonstrated reliable spatial measurement capabilities across diverse domains,[88–90], including clinical applications such as 3D laser scanning for foot plantar surface measurement. Although ToF systems may introduce error under certain conditions, particularly those linked to device positioning and surface reflectance, the error magnitudes recorded for OT-Vision remained well within the acceptable occupational therapy tolerances for pre-assessment activities.[18,34] These findings indicate that OT-Vision provides clinically acceptable levels of measurement bias whilst capitalising on the benefits associated with digital data capture.

In relation to measurement accuracy, OT-Vision demonstrated significantly lower absolute measurement error than the booklet for some measurement items, while the booklet did not significantly outperform OT-Vision in any case. After correction for multiple comparisons, this advantage remained statistically significant for two items (Bed Height and Chair Depth); the differences for Bath Internal Width, Chair Height, and Chair Width did not survive correction, indicating a more modest overall accuracy advantage than the uncorrected analysis suggested.

This pattern contrasts with that reported for the earlier, uncorrected PilOT-Measure pilot system,[29] in which the paper-based booklet was the more consistently accurate tool for the majority of measured items. The reversal of this pattern in the present study, following the introduction of the PPCDM correction algorithm, provides preliminary evidence that explicitly aligning measurement markers with detected object edges, rather than relying on uncorrected proximity to the raw point cloud, appears to meaningfully improve measurement accuracy in mobile depth-sensing applications of this kind.

Reduced accuracy was observed for measurements involving reflective surfaces, such as baths and toilets. This outcome is consistent with known limitations of ToF sensing, where glossy or translucent materials can result in sparsely populated or noisy depth data due to signal scattering. Analysis of OT-Vision's point-cloud outputs confirmed reduced depth density in these areas. While preprocessing steps, such as depth-map generation prior to edge filtering, mitigated some of these effects, challenges remained. Similar limitations have been reported in prior depth-sensing research, which highlights the importance of user scanning behaviour and environmental conditions when capturing accurate depth data.[91–93] These findings indicate that further optimisation of measurement marker placement and depth-map population is required to improve accuracy on reflective surfaces.

The task completion time results point to some efficiency gains associated with OT-Vision. Participants completed measurements significantly faster in the majority of cases, with particularly notable time savings for large or physically demanding measurements such as bath and stair length. Overall, OT-Vision reduced total task duration by several minutes compared with the booklet. Beyond direct time savings, the digital nature of OT-Vision removes the need for manual transcription and post-visit consolidation of paper records. This finding aligns with existing research highlighting the administrative and resource costs associated with paper-based HEFRA processes[94–96] and the potential for digital tools to streamline documentation and information flow.[97–99] Consistent with Tele-OT and health technology literature, the ability to generate a centralised, shareable digital assessment record may also support inter-professional collaboration and continuity of care.[25,100–107] In addition, OT-Vision has the potential to support broader clinical workflows beyond point-of-care measurement. As the system matures, integration with Electronic Health Record (EHR) systems and existing clinical workflows could enable automatic transfer of measurement data and depth-captured visual evidence, reducing duplicate data entry, supporting continuity of care, and facilitating information sharing across multidisciplinary teams. Furthermore, the ability to stream 3D point cloud data and depth-captured assessments to remote OTs could enable asynchronous or real-time collaborative decision-making, extending specialist assessment capacity beyond geographical constraints and addressing an important limitation of current Tele-OT practice. Future research should evaluate the technical feasibility, interoperability, and clinical utility of these integrations to determine their impact on service delivery and patient care.

Findings relating to usability and user experience further support the feasibility of OT-Vision as a clinical tool. OT-Vision achieved a higher mean SUS score than the booklet, with participants reporting lower perceived complexity, reduced awkwardness of use, and greater overall satisfaction. These findings are consistent with research suggesting that well-designed digital tools can enhance clinician interaction with assessment processes when compared with static paper-based

systems.[108] Nonetheless, some concerns were raised regarding interaction consistency and user confidence, particularly when marker placement was perceived as unreliable. These usability issues closely mirror the measurement accuracy challenges observed for reflective surfaces, suggesting that improvements in depth interpretation and visual feedback may simultaneously enhance both performance and user experience.

Clinicians' qualitative accounts provide further insight into perceived performance benefits, particularly in relation to reduced cognitive and administrative workload. Participants emphasised the value of integrating measurement guidance, digital records, and visual evidence within a single application, echoing findings from prior research on digitalising assessment practices in occupational therapy and related healthcare domains.[25,107] These perceived benefits were also linked to reduced stress during assessments, as shorter visits and simplified documentation were seen as advantageous for both practitioners and patients.[108]

Themes associated with ease of use and interaction effort suggested that participants experienced reduced manual effort and increased efficiency when using OT-Vision, reflecting benefits that have been reported in relation to the NHS Going Paperless agenda.[5,28,109,110] Suggested enhancements to the application included perpendicular measurement aids, adjustable marker opacity, and marker size controls. Such refinements align with broader UX research and material design considerations in 3D and augmented environments, which emphasise the importance of clear visual cues and interaction affordances.[111–117] Addressing these factors may further improve both measurement accuracy and clinician confidence.

Adoption-related insights emphasised the role of social and organisational influences. Participants identified age, experience, and professional culture as factors shaping openness to new technologies, with clinical leadership viewed as particularly influential in legitimising adoption. These observations align closely with established technology acceptance research, which highlights the importance of social endorsement, organisational readiness, and perceived legitimacy in driving uptake.[118,119] As such, successful deployment of OT-Vision is likely to depend not only on technical refinement, but also on training, leadership support, and organisational alignment.

6.1 Limitations

A further limitation of this study relates to the evaluation environment. Although the assisted daily living simulation setting enabled a high degree of standardisation and allowed direct comparison between OT-Vision and the paper-based guidance, it does not fully reflect the complexity, variability, and unpredictability of real patient homes and the diverse environmental conditions encountered in routine clinical practice. Factors such as differing property layouts, lighting conditions, clutter, user behaviours, and environmental constraints may influence both measurement performance and usability in routine practice. Consequently, the findings should be interpreted as evidence of the feasibility and performance of OT-Vision under controlled conditions rather than as a demonstration of effectiveness within routine clinical practice. Further evaluation in real domestic settings is therefore required to establish the ecological validity, clinical utility, and broader implementation potential of the application. Furthermore, the study did not involve assessments conducted with patients in their own homes, and therefore did not capture factors such as patient mobility limitations, cognitive impairment, caregiver involvement, or other contextual influences that may affect the practical use of the application. Future studies should evaluate OT-Vision within authentic clinical encounters to determine its applicability across a broader range of patient populations and care contexts.

The participant sample comprised both trainee and practising occupational therapists, introducing variability in levels of clinical experience and familiarity with assessment procedures. While this diversity reflects the range of potential users who may engage with OT-Vision in practice, it may also have influenced measurement performance, task completion times, and perceptions of usability. For example, practising clinicians may have benefited from greater familiarity with HEFRA processes, whereas trainees may have approached tasks with different levels of procedural knowledge and confidence. Similarly, individual differences in digital literacy and prior exposure to mobile technologies may have affected user interactions with the application. Consequently, the findings should be interpreted as representing aggregate performance across a heterogeneous user group rather than the experiences of a single professional cohort. Future research should investigate whether clinical experience, professional role, and digital competence influence the adoption, usability, and effectiveness of depth-enabled assessment tools. In addition, the study was designed to evaluate measurement performance, efficiency, and user experience, and did not assess clinical decision-making, patient outcomes, or falls risk reduction. Consequently, no clear conclusions can be drawn regarding the impact of OT-Vision on these outcomes, which warrant investigation in future real-world and longitudinal studies.

A further methodological consideration is that reference values were established through independent measurements undertaken by five experienced occupational therapists, with a single representative value agreed through expert consensus. Whilst this consensus reference standard was intended to minimise individual measurement bias and reflect established practice, formal inter-rater and intra-rater reliability analyses were beyond the scope of the present study. Future work

could evaluate measurement repeatability both within and between users and, where feasible, compare measurements against independent objective reference methods.

A further methodological consideration is that the study was conducted without participant blinding. Given the visible and functional differences between an interactive digital application and paper-based guidance, participant blinding to assessment modality was not feasible. This may have influenced subjective usability ratings, participant perceptions, and engagement. However, the paper-based guidance represented an established evidence-based comparator and was therefore an appropriate benchmark for evaluating OT-Vision against current practice. Future studies could reduce potential expectation or contrast effects through complementary study designs, such as between-subjects comparisons, assessor blinding where feasible, and greater use of objective performance outcomes.

ToF depth sensors offer a practical and low-cost means of capturing indoor 3D structure, but they have well-established limitations including reduced accuracy on reflective surfaces, performance degradation under challenging lighting, and artefacts near discontinuities and occlusions. Whilst a systematic evaluation of error distribution and performance under varying environmental conditions, including reflective surfaces, variable lighting, occlusion, and clutter, would provide additional insight into the robustness of the application, such testing was beyond the scope of this study, which was intentionally conducted under controlled laboratory conditions, and is acknowledged as a limitation and an important direction for future research. The findings should therefore be interpreted within the domain of occupational therapy home assessment and fall risk evaluation, where empirically derived acceptable measurement tolerances of 6–50 mm have been established.[14] Future depth-sensing systems intended for occupational therapy applications should be designed to minimise measurement error and be evaluated with respect to these clinically meaningful tolerance limits across a broader range of real-world environmental conditions to ensure relevance and interpretability.

6.2 Future research directions

Taken together, the findings indicate that OT-Vision offers a promising digital alternative to paper-based HEFRA measurement guidance within a controlled evaluation setting. The application demonstrated broadly comparable measurement bias, lower absolute measurement error for selected tasks, improved efficiency, and generally positive usability, while also revealing specific technical and interaction challenges that warrant further investigation. Further research is required to evaluate the performance, usability, and clinical utility of OT-Vision in routine home-based practice. Building on these findings, several directions for future research are identified:

1. *Clinical deployment and real-world utility* Evaluating OT-Vision within routine HEFRA practice to assess its impact on clinical decision-making, workflow integration, and patient outcomes.
2. *User-centric depth-sensing interaction strategies* Investigating how scanning behaviours, device handling, and movement patterns influence measurement bias and measurement accuracy in domestic environments.
3. *Interface and marker placement enhancements* Exploring design features such as perpendicular measurement aids, adaptive marker opacity, and adjustable marker size to reduce interaction effort and improve measurement accuracy.
4. *Improving performance on reflective and glossy surfaces* Developing and testing techniques to enhance depth capture and measurement reliability on shiny materials commonly found in bathrooms and kitchens.
5. *Adoption, training, and organisational readiness*
6. Examining how professional culture, leadership support, and training approaches influence clinicians' willingness to adopt depth-enabled HEFRA tools in practice.
7. *Depth-sensing enabled Tele-OT integration* Evaluating clinical utility of streaming 3D point cloud data to remote OTs for collaborative decision-making, including data protocols and electronic health records integration.

7 Conclusions

This study introduced OT-Vision, a point-to-point mobile measurement application utilising depth perception technology, developed with the goal of enabling occupational therapists to undertake digital HEFRAs with greater efficiency whilst maintaining or improving measurement accuracy. Within the context of a controlled assisted daily living simulation environment, OT-Vision demonstrated favourable outcomes across measurement bias, measurement accuracy, task completion time, and user satisfaction, performing comparably to the paper-based approach with respect to measurement bias, whilst demonstrating lower absolute measurement error for selected measurement tasks together with advantages in task completion time and user satisfaction. It should be noted that, following correction for multiple statistical comparisons, the measurement accuracy advantage remained statistically significant for only two measurement items. Nevertheless, no measurement item significantly favoured the paper-based booklet, and the overall pattern of findings remained favourable to

OT-Vision. Participants were receptive to adopting the application in their practice, acknowledging its capacity to streamline the assessment process and reduce delays. Whilst these findings provide evidence of the feasibility and performance of OT-Vision under controlled conditions, further evaluation in real-world home environments is required before conclusions can be drawn regarding its influence on clinical workflows, decision-making, and patient-related outcomes. These findings open several avenues for future research. Primary development efforts will concentrate on improving the precision and reliability of the marker placement function. Whilst the current study centres on clinician experiences of OT-Vision within the HEFRA workflow, the encouraging results indicate potential for wider application. Future work will examine the viability of deploying OT-Vision as a patient-facing self-assessment tool, as well as evaluating its performance in real-world settings and its potential effects on service efficiency and resource utilisation. This direction aligns with policy commitments to harnessing technology for more efficient, inclusive, and collaborative healthcare provision; however, the present study did not assess the impact of OT-Vision on falls risk, clinical outcomes, or healthcare costs, and based on the findings, these areas warrant further investigation.

Acknowledgements

The authors wish to express their gratitude to all participants who contributed to this study.

Ethical approval and participant consent

Ethical approval for this study was granted by Brunel University of London, College of Engineering, Design and Physical Sciences Research Ethics Committee Reference: 18844-LR-20747-1. Written informed consent was obtained from all participants prior to their involvement. All participants were advised that withdrawal from the study was permitted at any point without consequence.

Consent for publication

Not applicable.

Authors' contributions

ZI and AM conceptualised the study. Study planning and experimental design were led by ZI and AM and contributed to by AA and GS. ZI was responsible for application development. ZI conducted the user trials. Data analysis and manuscript preparation were carried out by ZI and AM. Subsequent manuscript revisions were reviewed and edited by ZI, AM, AA, and GS.

Funding

The authors received no financial support for the research, authorship, and/or publication of this article.

Declaration of conflicting interests

The authors declared no potential conflicts of interest with respect to the research, authorship, and/or publication of this article.

Availability of data and materials

Data used and/or analysed are obtainable from the corresponding author upon request.

ORCID iD

Arthur G Money https://orcid.org/0000-0003-1063-3680

References

1. Rudnicka E, Napierała P, Podfigurna A, et al. The World Health Organization (WHO) approach to healthy ageing. *Maturitas* 2020; 139: 6–11.
2. Jarman CH. Managing an ageing population lessons the UK could learn from Cuba. *Int J Cuban Stud* 2022; 14: 154–176.
3. Dixon J, Hurst J, Smith J, et al. *Can NHS hospitals do more with less?* Nuffield Trust, 2016, pp.1–92.
4. Horrell J, Lloyd H, Sugavanam T, et al. Creating and facilitating change for Person-Centred Coordinated Care (P3C): the development of the Organisational Change Tool (P3C-OCT). *Health Expect.* 2018; 21: 448–456.
5. Hunt J. Department of, NHS challenged to go paperless by 2018. 2013.
6. NHS England. NHS England Funding and Resource 2018/19: Supporting 'Next Steps for the NHS Five Year Forward View'. Public Policy, 2018: p. 1–10.
7. NHS. The NHS Long Term Plan. 2019. Available at: https://webarchive.nationalarchives.gov.uk/ukgwa/20230418155402/https://www.longtermplan.nhs.uk/publication/nhs-long-term-plan/.
8. NHS and A. Pritchard. NHS Long Term Workforce Plan. 2023. Available at: https://www.england.nhs.uk/wp-content/uploads/2023/06/nhs-long-term-workforce-plan-v1.2.pdf.

9. Office for Health Improvement and Disparities. Falls: applying All Our Health. Public Policy, 2022, pp.1–12.
10. Logan PA, Coupland CAC, Gladman JRF, et al. Community falls prevention for people who call an emergency ambulance after a fall: randomised controlled trial. *Br Med J.* 2010; 340: c2102.
11. Atwal A, Mcintyre A, Spiliotopoulou G, et al. Disability and rehabilitation: assistive technology How are service users instructed to measure home furniture for provision of minor assistive devices? 2016.
12. Spiliotopoulou G. National guidance for measuring home furniture and fittings to enable user self-assessment and successful fit of minor assistive devices Key findings. 2016.
13. Spiliotopoulou G. Brunel University Home Furniture Measurement. 2022. Available at: https://www.independentliving.co.uk/Brunel-measurement-guidance.pdf.
14. Spiliotopoulou G, Atwal A and McIntyre A. The use of evidence-based guidance to enable reliable and accurate measurements of the home environment. *Br J Occup Ther.* 2018; 81: 32–41.
15. Riemer-Reiss ML and Wacker RR. Factors associated with assistive technology discontinuance among individuals with disabilities. *J Rehabil.* 2000; 66: 44–50.
16. Federici S, Meloni F and Borsci S. The abandonment of assistive technology in Italy: a survey of users of the national health service. *Eur J Phys Rehabil Med.* 2016; 52: 516–526.
17. Hamm J, Money AG, Atwal A, et al. Mobile three-dimensional visualisation technologies for clinician-led fall prevention assessments. *Health Informatics J.* 2019; 25: 788–810.
18. Hamm J, Money A and Atwal A. Guidetomeasure-OT: a mobile 3D application to improve the accuracy, consistency, and efficiency of clinician-led home-based falls-risk assessments. *Int J Med Inf.* 2019; 129: 349–365.
19. Verza R, Carvalho MLL, Battaglia MA, et al. An interdisciplinary approach to evaluating the need for assistive technology reduces equipment abandonment. *Mult Scler J* 2006; 12: 88–93
20. Goodacre K, McCreadie C, Flanagan S, et al. Enabling older people to stay at home: the costs of substituting and supplementing care with assistive technology. *Br J Occup Ther* 2008; 71: 130–140.
21. Money AG, Atwal A, Young KL, et al. Using the Technology Acceptance Model to explore community dwelling older adults' perceptions of a 3D interior design application to facilitate pre-discharge home adaptations. *BMC Med Inform Decis Mak.* 2015; 15: 73.
22. Amy Jang A, MacLean DL and Heer J. Bodydiagrams: improving communication of pain symptoms through drawing. In: Proceedings of the SIGCHI conference on human factors in computing systems. ACM, 2014, pp.1153–1162.
23. Money AG, Atwal A, Boyce E, et al. Falls Sensei: a serious 3D exploration game for older adults to enable the detection of extrinsic fall hazards within the home. *BMC Med Inform Decis Mak.* 2019; 19: 85.
24. Ibrahim Z and Money AG. Computer mediated reality technologies: a conceptual framework and survey of the state of the art in healthcare intervention systems. *J Biomed Inform.* 2019; 90: 103102–103102.
25. Hamm J, Money AG and Atwal A. Enabling older adults to carry out paperless falls-risk self-assessments using guidetomeasure-3D: a mixed methods study. *J Biomed Inform.* 2019; 92: 103135–103135.
26. Money AG, Mcintyre A, Atwal A, et al. *Bringing the home into the hospital: Assisting the pre-discharge home visit process using 3D home visualization software*. Springer, 2011.
27. Hamm J, Money AG and Atwal A. Fall prevention self-assessments via Mobile 3D visualization technologies: community dwelling older Adults' perceptions of opportunities and challenges. *JMIR Hum Factors.* 2017; 4: e15.
28. Nix J and Comans T. Home quick - occupational therapy home visits using mHealth, to facilitate discharge from acute admission back to the community. *Int J Telerehabil.* 2017; 9: 47–54.
29. Ibrahim Z, Money AG., Atwal A, et al. PilOT-Measure: a mobile 3D depth sensing application to support accurate and efficient clinician-led home-based falls risk assessments. *BMC Med Inform Decis Mak.* 2025; 25: 332.
30. Google. ARCore: Dynamic Depth. 2019 June, 2026]. Available at: https://developer.android.com/training/camera2/Dynamic-depth-v1.0.pdf.
31. Luetzenburg G, Kroon A and Bjørk AA. Evaluation of the Apple iPhone 12 Pro LiDAR for an application in geosciences. *Sci Rep.* 2021; 11: 22221.
32. Jing C, Potgieter J, Noble F, et al. A comparison and analysis of RGB-D cameras' depth performance for robotics application. In: *2017 24th international conference on mechatronics and machine vision in practice (M2VIP)*, 2017.
33. Nguyen KA and Luo Z. On assessing the positioning accuracy of Google Tango in challenging indoor environments. In: International conference on indoor positioning and indoor navigation (IPIN). IEEE, 2017.
34. Roberto R, Lima J, Araujo T, et al.Evaluation of motion tracking and depth sensing accuracy of the Tango tablet. In: *IEEE international symposium on mixed and augmented reality (ISMAR-adjunct)*. Institute of Electrical and Electronics Engineers Inc, 2016.
35. Kalantari M and Nechifor M. Accuracy and utility of the structure sensor for collecting 3D indoor information. *Geo-Spat Inf Sci* 2016; 19: 202–209.

36. Occipital. Structure Sensor Depth Precision. 2016.
37. Huawei. HUAWEI AR Engine - Overview. 2019. Available at: https://developer.huawei.com/consumer/en/doc/overview/HMS.
38. Kamińska MS, Miller A, Rotter I, et al. The effectiveness of virtual reality training in reducing the risk of falls among elderly people. *Clin Interv Ageing* 2018; 13: 2329–2338.
39. Yang CM, Chen Hsieh J, Chen YC, et al. Effects of Kinect exergames on balance training among community older adults. *Medicine (Baltimore).* 2020; 99: e21228.
40. Hsieh WM, Chen CC, Wang SC, et al. Virtual reality system based on Kinect for the elderly in fall prevention. *Technol Health Care.* 2014; 22: 27–36.
41. Dutta A, Chugh S, Banerjee A, et al. Point-of-care-testing of standing posture with Wii balance board and Microsoft Kinect during transcranial direct current stimulation: a feasibility study. *NeuroRehabilitation* 2014; 34: 789–798.
42. Pu F, Sun S, Wang L, et al. Investigation of key factors affecting the balance function of older adults. *Aging Clin Exp Res.* 2015; 27: 139–147.
43. Gama AD, Chaves T, Figueiredo L, et al. *Guidance and movement correction based on therapeutics movements for motor rehabilitation support systems*. IEEE, 2012.
44. Stone EE and Skubic M. Fall detection in homes of older adults using the Microsoft Kinect. *IEEE J Biomed Health Inform.* 2015; 19: 290–301.
45. Ibrahim Z. OT-Vision Application Source Code. [C#, Unity, Tango] 2025; A Mobile Depth Sensing and Motion Tracking Device application to support Occupational Therapists in the process of capturing extrinsic measurements for the Home-Environment and Falls-Prevention Process.]. Available at: https://github.com/zearibrahim/ot-vision/releases/tag/1.0.
46. Apple. iPhone 12 Pro Technical Specification. 2020 June, 2026]. Available at: https://support.apple.com/en-gb/111875.
47. Apple. iPhone 15 Pro Max Technical Spec TrueDepth LiDAR Camera. 2023 June, 2026]. Available at: https://support.apple.com/en-gb/111828.
48. Huawei. (Primary) P30 Pro Technical Features - ToF Depth Camera and 3D True Depth. 2023 June, 2026]. Available at: https://consumer.huawei.com/en/community/details/topicId-5450/.
49. Huawei. (Secondary) P30 Pro Technical Features - ToF Depth Camera and 3D True Depth. 2023 June, 2026]. Available at: https://www.gsmarena.com/huawei_p30_pro-9635.php.
50. Huawei. (Primary) P40 Pro Technical Specifcation - With 3D Depth Sensing Camera. 2020 June, 2026]. Available at: https://consumer.huawei.com/ke/phones/p40-pro/specs/.
51. Huawei. (Secondary) P40 Pro Technical Specifcation - With 3D Depth Sensing Camera. 2020 June, 2026]. Available at: https://www.gsmarena.com/huawei_p40_pro-10152.php.
52. Samsung. (Primary) Galaxy S20 Ultra - Technical Specification. 2020 June, 2026]. Available at: https://www.samsung.com/levant/smartphones/galaxy-s20/specs/.
53. Samsung. (Secondary) Galaxy S20 Ultra - Technical Specification TOF Depth. 2020 June, 2026]. Available at: https://www.gsmarena.com/samsung_galaxy_s20_ultra_5g-10040.php.
54. Samsung. (Primary) Galaxy A80 - Technical Specification. 2023 June, 2026]. Available at: https://news.samsung.com/global/new-samsung-galaxy-a80-built-for-the-era-of-live.
55. Samsung. (Secondary) Galaxy A80 - Technical Specification. 2023 June, 2026]. Available at: https://www.gsmarena.com/samsung_galaxy_a80–9659.php.
56. Gsmarena. List of Mobile Phones with ToF Depth Sensors. 2023 June, 2026]. Available at: https://www.gsmarena.com/results.php3?sFreeText=TOF.
57. Ghali S. *Homogeneous coordinates for Euclidean geometry*. Springer London, 2008, pp.171–174.
58. Stearns CC and Kannappan K. Method for 2-D affine transformation of images. 1995. pp.1–17.
59. Mure-Dubois J, Charles C, Heinz H, et al. Fusion of time of flight camera point clouds fusion of time of flight camera point clouds. In: *Workshop on multi-camera and multi-modal sensor fusion algorithms and applications-M2SFA2 2008 fusion of time of flight camera point clouds*, 2008.
60. Hansard M, Evangelidis G, Pelorson Q, et al. Cross-calibration of time-of-flight and colour cameras. *Comput Vis Image Underst.* 2015; 134: 105–115.
61. Hansard M, Lee S, Choi O, et al. *Time of flight cameras: principles, methods, and applications*. SpringerBriefs in Computer Science. Springer London, 2012, p.95.
62. Apple. ARKit: Get ready for the latest advances in augmented reality. 2019 June, 2026]. Available at: https://developer.apple.com/augmented-reality/.
63. Huawei. AR Engine - PointCloud Structure. 2019 June, 2026]. Available at: https://developer.huawei.com/consumer/en/doc/development/HMSCore-References-V5/point_cloud-0000001050119504-V5.
64. Scratchpixel. Computing the Pixel Coordinates of a 3D Point. 2016 June, 2026]. Available at: http://www.scratchapixel.com/lessons/3d-basic-rendering/computing-pixel-coordinates-of-3d-point/mathematics-computing-2d-coordinates-of-3d-points.

65. Jiang H, Tian Q, Farrell J, et al. Learning the image processing pipeline. *IEEE Trans Image Process.* 2017; 26: 5032–5042.
66. Ganapathy S. Decomposition of transformation matrices for robot vision. *Pattern Recognit Lett.* 1984; 2: 401–412.
67. Gohlke C. 4×4 Matrix Transformations. 2020, Laboratory for Fluorescence Dynamics. University of California, Irvine.
68. Dandekar K, Raju BI and Srinivasan MA. 3-D finite-element models of human and monkey fingertips to investigate the mechanics of tactile sense. *J Biomech Eng.* 2003; 125: 682–691.
69. Google. Project Tango Data Handling. 2026 [cited July, 2026. Available at: https://support.google.com/faqs/answer/6122425?hl=en.
70. Fu Y, Zhou C, Ye H, et al. FractalCloud: a fractal-inspired architecture for efficient large-scale point cloud processing. In: *2026 IEEE international symposium on high performance computer architecture (HPCA)*, 2026.
71. Roriz R, Silva H, Dias F, et al. A survey on data compression techniques for automotive LiDAR point clouds. *Sensors* 2024; 24: 3185.
72. Microsoft C, Sullivan G and Estrop S. FOURCC Codes. Windows Development Center, 2018.
73. Microsoft C. Recommended 8-Bit YUV Formats for Video Rendering. Microsoft Corporation, 2018,.
74. King DB, O'Rourke N and DeLongis A. Social media recruitment and online data collection: a beginner's guide and best practices for accessing low-prevalence and hard-to-reach populations. *Can Psychol* 2014; 55: 240–249.
75. Pollard N and Walsh S. Occupational therapy, gender and mental health: an inclusive perspective? *Br J Occup Ther.* 2000; 63: 425–431.
76. Beagan BL and Fredericks E. What about the men? Gender parity in occupational therapy. *Can J Occup Ther.* 2018; 85: 137–145.
77. Versi E. "Gold standard" is an appropriate term. *Br Med J.* 1992; 305: 187–187.
78. Bertens LCM, Broekhuizen BDL, Naaktgeboren CA, et al. Use of expert panels to define the reference standard in diagnostic research: a systematic review of published methods and reporting. *PLoS Med* 2013; 10: e1001531.
79. Reitsma JB, Rutjes AWS, Khan KS, et al. A review of solutions for diagnostic accuracy studies with an imperfect or missing reference standard. *J Clin Epidemiol* 2009; 62: 797–806.
80. Bangor A, Kortum P and Miller J. Determining what individual SUS scores mean: adding an adjective rating scale. *J Usability Stud.* 2009; 4: 114–123.
81. George D and Mallery P. *IBM SPSS statistics 27 step by step: a simple guide and reference*. 17th ed. Routledge, 2021.
82. Marks D and Yardley L. *Research methods for clinical and health psychology*. Sage, 2004.
83. Virginia B and Victoria C. One size fits all? What counts as quality practice in (reflexive) thematic analysis? *Qual Res Psychol.* 2020; 18: 328–352.
84. Crabtree B and Miller W. A template approach to text analysis: developing and using codebooks. In: *Doing qualitative research in primary care: multiple strategies*. Sage Publications, 1992, pp.93–109.
85. Fereday J and Muir-Cochrane E. Demonstrating rigor using thematic analysis: a hybrid approach of inductive and deductive coding and theme development. *Int J Qual Methods.* 2006; 5: 80–92.
86. Venkatesh V, Morris MG, Davis GB, et al. User acceptance of information technology: toward a unified view 1. *MIS Q.* 2003; 27: 425–478.
87. Ellem K. Doing qualitative research in social work. *Aust Soc Work* 2015; 68: 402–403.
88. Kalyan TS, Zadeh PA, Staub-French S, et al. Construction quality assessment using 3D as-built models generated with project Tango. *Procedia Eng.* 2016; 145: 1416–1423.
89. Gulch E. *Investigations on Google Tango development kit for personal indoor mapping*. AGILE, 2016.
90. Froehlich M, Azhar S and Vanture M. An Investigation of Google Tango ® Tablet for Low Cost 3D Scanning. 2017.
91. Zumtobel. *The lighting handbook: your concise reference book*. Zumtobel Lighting GmbH, 2017, pp.230–230.
92. Kaufmann M. In: Poynton C (ed) *Algorithms and interfaces*. Elsevier, 2012, pp.709–709.
93. Nejati H, Pomponiu V, Do TT, et al. Smartphone and mobile image processing for assisted living: health-monitoring apps powered by advanced mobile imaging algorithms. *IEEE Signal Process Mag.* 2016; 33: 30–48.
94. Nagayama H, Tomori K, Ohno K, et al. Cost-effectiveness of occupational therapy in older people: systematic review of randomized controlled trials. *Occup Ther Int.* 2016; 23: 103–120.
95. Zingmark M, Nilsson I, Fisher AG, et al. Occupation-focused health promotion for well older people-A cost-effectiveness analysis. *Br J Occup Ther.* 2016; 79: 153–162.
96. De Coninck L, Bekkering GE, Bouckaert L, et al. Home- and community-based occupational therapy improves functioning in frail older people: a systematic review. *J Am Geriatr Soc.* 2017; 65: 1863–1869.
97. Shamus E, Fabrizi S and Hogan J. A qualitative study of professional issues in home health therapy. *Home Health Care Manag Pract* 2018; 30: 9–15.
98. Sampson C, James M, Whitehead P, et al. An introduction to economic evaluation in occupational therapy: cost-effectiveness of pre-discharge home visits after stroke (HOVIS). *Br J Occup Ther.* 2014; 77: 330–335.

99. Atwal A, Spiliotopoulou G, Stradden J, et al. Factors influencing occupational therapy home visit practice: a qualitative study. *Scand J Occup Ther.* 2014; 21: 40–47.
100. Hung Kn G and Fong KN. Effects of telerehabilitation in occupational therapy practice: a systematic review. Hong Kong journal of occupational therapy. *Hong Kong J Occup Ther* 2019; 32: 3–21.
101. Cason J. Telehealth: a rapidly developing service delivery model for occupational therapy. *Int J Telerehabil.* 2014; 6: 29–36.
102. Bendixen RM, Levy CE, Olive ES, et al. Cost effectiveness of a telerehabilitation program to support chronically ill and disabled elders in their homes. *Telemed e-Health* 2009; 15: 31–38.
103. Garg AX, Adhikari NKJ, McDonald H, et al. Effects of computerized clinical decision support systems on practitioner performance and patient outcomes. *JAMA* 2005; 293: 1223–1223.
104. Forsman J, Anani N, Eghdam A, et al. Integrated information visualization to support decision making for use of antibiotics in intensive care: design and usability evaluation. *Inform Health Soc Care* 2013; 38: 330–353.
105. De Georgia MA, Kaffashi F, Jacono FJ, et al. Information technology in critical care: review of monitoring and data acquisition systems for patient care and research. *Scientific World J.* 2015; 2015: 1–9.
106. Lin YL, Trbovich P, Kolodzey L, et al. Association of data integration technologies with intensive care clinician performance: a systematic review and meta-analysis. *JAMA Netw. Open.* 2019; 2: e194392–e194392.
107. Ninnis K, Van Den Berg M, Lannin N, et al. *Information and communication technology use within occupational therapy home assessments: a scoping review*. Sage Publications Inc, 2019, pp.141–152.
108. Read J, Jones N, Fegan C, et al. Remote home visit: exploring the feasibility, acceptability and potential benefits of using digital technology to undertake occupational therapy home assessments. *Br J Occup Ther.* 2020; 83: 648–658.
109. National-Health-Service, et al. Five Year Forward View. 2014 22/05/2017]. Available at: https://www.england.nhs.uk/wp-content/uploads/2014/10/5yfv-web.pdf.
110. Atwal A, Money A and Harvey M. Occupational therapists' views on using a virtual reality Interior design application within the Pre-discharge home visit process. *J Med Internet Res.* 2014; 16: e283–e283.
111. Bergé LP, Dubois E, Houry-Panchetti M, et al. Towards an engineering approach for advanced interaction techniques in 3D environments. In: *ACM SIGCHI*, 2014.
112. Shi W, Wang Z, Sezgin M, et al.. Material design in augmented reality with in-situ visual feedback. In: *Proceedings of the eurographics symposium on rendering: experimental ideas & implementations*. Eurographics Association, 2017, pp.93–103.
113. Zhu E, Lilienthal A, Shluzas LA, et al. Design of Mobile augmented reality in health care education: a theory-driven framework. *JMIR Med Educ.* 2015; 1: e10.
114. Chung CJ and Tuan HW. Applying virtual reality to design the game-based system for rehabilitation of artificial hip. In: ICIGP 2020: proceedings of the 2020 3rd international conference on image and graphics processing. 2020.
115. Liang S. Design principles of augmented reality focusing on the ageing population. In: HCI '16: proceedings of the 30th international BCS human computer interaction conference: fusion! 2016. BCS Learning and Development Ltd.
116. Han SH, Kim KJ, Yun MH, et al. Identifying mobile phone design features critical to user satisfaction. *Hum Factors Ergon Manuf Serv Ind* 2004; 14: 15–29.
117. Igler B. Feature evaluation for mobile applications: a design science approach based on evolutionary software prototypes. In: *DUXU 2013: design, user experience, and usability. Web, mobile, and product design*. Springer, 2013, pp.673–681.
118. Martín-García AV, Redolat R and Pinazo-Hernandis S. Factors influencing intention to technological use in older adults. The TAM model aplication. *Res Aging* 2021; 44: 573–588.
119. Guner H and Acarturk C. The use and acceptance of ICT by senior citizens: a comparison of technology acceptance model (TAM) for elderly and young adults. *Univer Access Inf Soc.* 2020; 19: 311–330.

Appendix A

The mathematical formulation of the proposed computer vision handler is presented in Section 2.3 of the main manuscript. The source-code for this can be found on GitHub[45]. This appendix provides the corresponding programming language-independent pseudocode. Each table has several points of interest ($\triangleleft$) which support reproducibility and facilitate re-implementation of the image-processing pipeline in alternative programming languages.

Table 5. PPCDM depth-map computation.

PSEUDO–CODE: DepthMapComputation <METHOD>, <Data Call–back>		
INPUT: raw_point_cloud [X,Y,Z,W], camera intrinsics (fx, fy, cx, cy, width, height)		
OUTPUT: A Depth Map List or Texture Image (+ coordinates)		
ACTIVATION: Device Data Call–back		
1	depthmap ← new VDCH(height × width)	◁ (1)
2		
3	for i = 0 → raw_point_cloud.count:	
4	(Ta_X, Ta_Y, Ta_Z) ← raw_point_cloud [i*4 : i*4 + 3]	◁ (2)
5		
6	Ca_x ← (fx * Ta_X/Ta_Z) + cx	◁ (3)
7	Ca_y ← (fy * Ta_Y/Ta_Z) + cy	◁ (4)
8		
9	if Ca_x < 0 or Ca_x ≥ width or Ca_y < 0 or Ca_y ≥ height:	◁ (5)
10	continue	
11		
12	Ca_z ← 255 - ((Ta_Z * 1000) * 255 / 4500)	◁ (6)
13	depthmap.add(Ca_x, Ca_y, i)	◁ (7)
14	end for	

Note: To maintain pseudocode clarity, we write in Ca_x format and denote C_{ax} in formulas.

Pseudocode: Depth-map computation

Table 5 presents the logic for the Depth Map Computation in Section 2.3.1.

At ◁ (1), we instantiate array storage for all depth map and point cloud points. At ◁ (2), individual point cloud vertices X, Y, Z are stored as homogeneous coordinates. At ◁ (3) and ◁ (4), the colour camera intrinsics are retrieved and implement Equations (4) and (5) to compute the projected depth map pixel values. At ◁ (5), results are validated against the image bounds. At ◁ (6), Equation (6) is adopted to compute depth at the given pixel. Finally, at ◁ (6), we store the pixel values and their corresponding point-cloud indices to lookup 3D edges later in Phase 2 (Sobel Convolution, Table 6).

Pseudocode: Sobel convolution

Table 6 presents the 3×3 Sobel convolution using a local-windowed search in Section 2.3.2.

At ◁ (1), the users Point Selection is used as the centre point for the window and defines our reduced iteration space. It applies an local window 100-pixel search frame (adjustable) based on tactical sensing research, where the average pointer finger size was 16–20 mm (45–57 pixels) and is doubled for effective touch-based experience[68]. At ◁ (2), we obtain the corresponding pixel index in the image plane using the RGB image buffer. At ◁ (3), we identify all neighbouring pixels. At ◁ (4), we apply the 3×3 kernel and at ◁ (5) we compute the gradient magnitude. At ◁ (6), we compare the magnitude to an adjustable edge threshold of 1024. A threshold of $t(1024)$ captures 2–5 pixel-wide edges. Denser edges can be extracted by doubling $t \rightarrow t \times 2$ or single line edges by halving $t \rightarrow t \div 2$. At ◁ (7), we lookup if this edge exists in the depth map, if it does, we mark it as a 3D edge and save the point cloud index.

Pseudocode: 2D to 3D edge and user point mapping

Table 7 presents the logic for the NNFRLS algorithm in Section 2.3.3.

The NNFRLS algorithm in Table 7 brings together the depth map, point cloud and user's touch input vector to find the nearest 3D edge. At ◁ (1), we retrieve the 3D edges based on the users touch vector. This step simply retrieves the depth map and the associated edges using the same 100-pixel search range as defined in Table 6. At ◁ (2), we iterate through each edge coordinate using a naïve linear search. At ◁ (3) we compute the squared distance between the normalised touch position and the current edge point. At ◁ (4), we check if the squared distance is within the maximum distance allowed and is smaller than the previously stored closest distance. If so, we update the best 3D edge array index and squared distance values. At ◁ (4) if an acceptable edge was found, the device vibrates, and the corresponding point-cloud value is returned for animation in the Measurement Application GUI; otherwise, −1 is returned.

Table 6. PPCDM sobel convolution and mapping.

PSEUDO–CODE: SobelConvolution <METHOD>

INPUT: image <RGB Buffer>, width, height, x_pixel, y_pixel, τ, edge_threshold, depthmap

OUTPUT: A list of edges OR texture image

ACTIVATION: Procedure/Function call

```
1     for j = (y_pixel - τ) → (y_pixel + τ - 1):                          ◁(1)
2       for i = (x_pixel - τ) → (x_pixel + τ - 1):
3
4         Cb_ij ← (j * width) + i                                         ◁(2)
5
6         p00 ← image [Cb_ij - width - 1]                                 ◁(3)
7         p01 ← image [Cb_ij - width]
8         p02 ← image [Cb_ij - width + 1]
9         p10 ← image [Cb_ij - 1]
10        p12 ← image [Cb_ij + 1]
11        p20 ← image [Cb_ij + width - 1]
12        p21 ← image [Cb_ij + width]
13        p22 ← image [Cb_ij + width + 1]
14
15        dx ← -p00 – 2*p10 - p20 + p02 + 2*p12 + p22                     ◁(4)
16        dy ← p00 + 2*p01 + p02 - p20 – 2*p21 - p22
17
18        m ← (dx^2 + dy^2)                                               ◁(5)
19
20        if m ≥ edge_threshold:                                          ◁(6)
21          idx ← depthmap.lookup(Cb_ij)                                  ◁(7)
22          if idx ≠ null:
23            depthmap.mark(Cb_ij, idx)
24      end for
25    end for
```

Note: To maintain pseudocode clarity, we write in Cb_ij format and denote $C_b(i,\ j)$ in formulas.

Table 7. PPCDM NNFRLS algorithm.

PSEUDO–CODE: PPCDM NNFRLS Algorithm

INPUT: camera_intrinsics, t_vector <user touch/screen coordinate space>, maxDist <PIXELS>

OUTPUT: Closest 3D edge point or –1 if none

ACTIVATION: On Touch–Event <SINGLE>, <DRAG>

```
1     b_index ← –1
2     b_sqr_distance ← ∞
3
4     norm_pos ← Normalise(t_vector, camera_intrinsics)
5     edge_list ← Get3DEdges(norm_pos, maxDist)                           ◁(1)
6
7     for each edge in edge_list:                                         ◁(2)
8       sqr_distance ← |norm_pos – edge.2d|^2                             ◁(3)
9       if sqr_distance ≤ maxDist^2 AND sqr_distance < b_sqr_distance:    ◁(4)
10        b_index ← edge.3d
11        b_sqr_distance ← sqr_distance
12    end for
13
14    if b_index ≠ –1:                                                    ◁(4)
15      VibrateDevice()
16      return b_index
17    else:
18      return –1
```

Table 8. Bland-Altman bias and non-parametric limits of agreement, OT-Vision vs. booklet.

Measurement item	n	Median difference (Bias, cm)	Non-parametric limits of agreement (2.5–97.5th percentile, cm)
Bath Height	37	0.77	[−2.64, 4.20]
Bath Internal Width	37	0.57	[−1.68, 8.74]
Bath Length	37	−0.27	[−8.66, 15.21]
Bath External Width	37	−0.09	[−3.21, 5.53]
Bed Height	37	−0.48	[−8.01, 12.92]
Chair Height	37	−0.41	[−8.10, 3.25]
Chair Depth	37	1.41	[−6.86, 6.24]
Chair Width	37	0.79	[−5.45, 5.87]
Toilet Height A (Floor–Seat)	37	0.89	[−3.32, 5.69]
Toilet Height B (Floor–Bowl)	37	0.73	[−2.52, 3.55]
Stairs Length	37	0.16	[−1.74, 4.11]

Appendix B

Bland-Altman analysis of measurement agreement

To further characterise the degree of agreement between OT-Vision and the paper-based booklet, Bland-Altman analyses were conducted for each of the eleven measurement items. For each item, the difference between the two tools' readings (OT-Vision minus booklet) was plotted against the mean of the two readings for each participant. As measurement error data did not satisfy normality assumptions elsewhere in this study, a non-parametric variant of the Bland-Altman approach was adopted: bias is reported as the median difference between tools, and limits of agreement are reported as the empirical 2.5th and 97.5th percentiles of the paired differences, rather than the mean $\pm$ 1.96 standard deviation formula, which assumes normally distributed differences. Results are summarised in Table 8 and Figure 10.

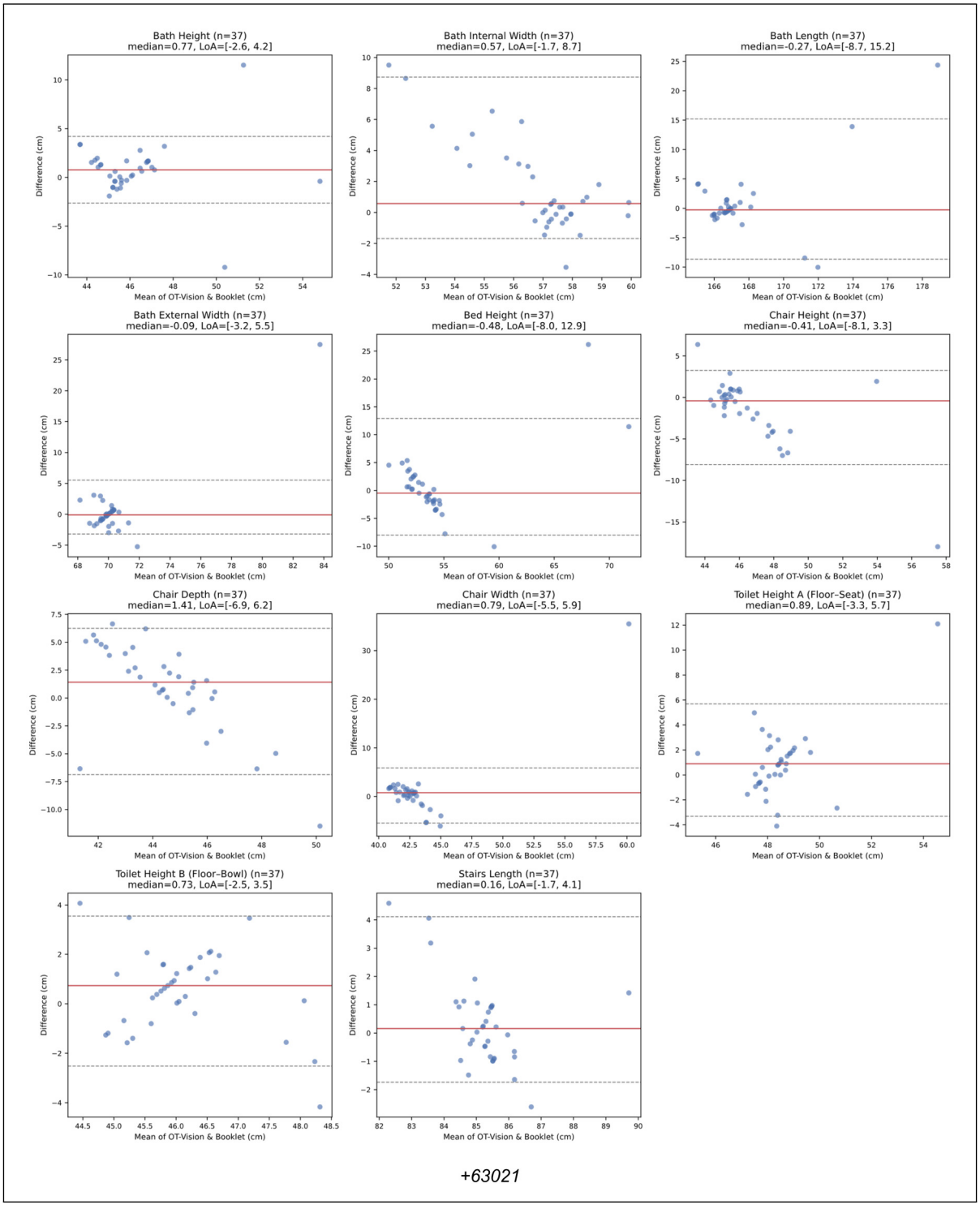


Figure 10. Geometric model of the PPCDM technique. Mobile depth sensor/camera frames (tTime of Flight and RGB) generate 4D homogeneous point-cloud through stereoscopic depth. 4D coordinates are de-homogenised using Translate Rotate and Scale functions (TRS).